Molecular basis of methyl salicylate-mediated plant airborne defense

Qian Gong[1,2,9], Yunjing Wang[1,2,9], Linfang He[1,2], Fan Huang[1,2], Danfeng Zhang[1,2], Yan Wang[1,2], Xiang Wei[1], Meng Han[3], Haiteng Deng[3], Lan Luo[4], Feng Cui[4], Yiguo Hong[5,6,7,8], Yule Liu[1,2*]

[1] MOE Key Laboratory of Bioinformatics and Center for Plant Biology, School of Life Sciences, Tsinghua University, Beijing 100084, China

[2] Tsinghua-Peking Center for Life Sciences, Beijing 100084, China

[3] Protein Research Technology Center Protein chemistry and omics Platform, School of Life Sciences, Tsinghua University, Beijing 100084, China

[4] State Key Laboratory of Integrated Management of Pest Insects and Rodents, Institute of Zoology, Chinese Academy of Sciences, Beijing, China

[5] State Key Laboratory of North China Crop Improvement and Regulation and College of Horticulture, Hebei Agricultural University, Baoding 071000, China

[6] Research Centre for Plant RNA Signaling, College of Life and Environmental Sciences, Hangzhou Normal University, Hangzhou 311121, China

[7] School of Life Sciences, University of Warwick, Coventry CV4 7AL, UK

[8] School of Science and the Environment, University of Worcester, Worcester WR2 6AJ, UK

[9] These authors contributed equally to this work

[*] Correspondence Author: yuleliu@mail.tsinghua.edu.cn (Y.L)

Abstract

Aphids transmit viruses and are destructive crop pests[1]. Aphid-attacked plants release volatile compounds to elicit airborne defense (AD) in neighboring plants[2-5]. However, the mechanism underlying AD is unknown. Here, we reveal methyl-salicylate (MeSA), salicylic-acid (SA)-binding protein-2 (SABP2), transcription factor NAC2, and SA-carboxylmethyltransferase-1 (SAMT1) form a signaling circuit to mediate AD against aphids and viruses. Airborne MeSA is perceived and converted to SA by SABP2 in neighboring plants. SA then cascades signal transduction to activate the NAC2-SAMT1 module for MeSA biosynthesis to induce plant anti-aphid immunity and reduce virus transmission. To counteract, some aphid-transmitted viruses encode helicase-containing proteins to suppress AD by interacting with NAC2 to subcellularly re-localize and destabilize NAC2. Consequently, plants become less aphid-repellent, but more suitable for aphid survival, infestation, and viral transmission. Our findings uncover mechanistic basis of AD and a previously undefined aphid-virus co-evolutionary mutualism, demonstrating AD as a potential bioinspired strategy to control aphids and viruses.

Main

Plants have evolved the capacity to sense environmental stimuli and induce changes of metabolism to generate volatile organic compounds (VOCs) as intra/interplant signals[2,6]. VOCs, once released from 'VOC emitter' plants, can serve as aerial cues and be perceived to elicit defenses in neighboring 'receiver' plants, a phenomenon called

airborne defense (AD)[2-5]. Such plant-plant communication (PPC) and its biological and ecological significance have been observed in many species over decades[2,3]. Very recently, UDP-arabinosyltransferase is found to be involved in airborne volatile reception in tomato distal defense against cutworms[7]. However, molecular genetic framework for the VOC-mediated PPC including AD is largely unknown[2]. Moreover, with the exception of the receptor for ethylene[8], the receptors for mediating VOC-sensing system in plants have remained unidentified.

Aphids are the most destructive agricultural and horticultural pests worldwide[1]. They are phloem-feeding and cause extensive destruction to crop production due to their efficient transmission of numerous devastating viral pathogens[1]. More than 40% viruses depend on aphids for transmission to infect plants including many food, fruit, and vegetable crops[9]. Aphid-attack induces plant emitting VOCs which are mainly composed of MeSA[10-13]. MeSA has been implicated in plant defense against herbivorous insects including aphids by repelling, attracting predators, or reducing survival fitness of these insects[14-16]. MeSA, known as a within-plant and long-distance mobile signal, is involved in inducing systemic acquired resistance (SAR) to microbial pathogens and herbivorous insects[17,18]. During SAR, SA accumulates in pathogen-infected cells and is converted to MeSA by SAMT1[19]; MeSA then travels to distal tissues via the phloem and is subsequently reconverted to SA by SABP2 for SAR in systemic leaves[20]. Although MeSA as a within-plant signal for SAR is known, how MeSA serves as an interplant communication signal to activate anti-aphid defense in neighboring 'receiver' plants has been a long-standing and unsolved question[2,10,16]. For

instance, whether plants possess receptor systems to sense and perceive airborne MeSA is unclear[3]. Mechanism for priming MeSA production during aphid infestation is also not illuminated. Furthermore, it remains to be elucidated whether and how aphids and viruses can regulate AD although MeSA is reported to mediate AD against *Tobacco mosaic virus* (TMV, a Tobamovirus in the family *Virgaviridae*)[4]. In this study, we have exploited a pathosystem comprising aphid, virus, VOC emitter, and receiver plants to dissect AD. We establish the framework for MeSA mediating AD to suppress insect infestation and virus transmission at molecular and genetic level, and identified an odorant-binding protein (OBP)-like receptor for sensing and perceiving airborne MeSA. Further, we found an unexpected viral counterdefense strategy to suppress plant AD, suggesting an undefined ecological and co-evolutionary mutualism between aphids and aphid-transmissible viruses. Moreover, our findings lay the groundbreaking work to provide the detailed mechanism of VOC-triggered PPC and will pave the way for future studies on PPC and plant adaptation to environment.

Plant antiviral defense requires NAC2

Following our work on *Cucumber mosaic virus* (CMV), a Cucumovirus in the family *Bromoviridae*[21], we investigated the role of CMV 1a protein (designated CMV1a hereafter) in viral pathogenesis. Through conducting immuno-pulldowns coupled with mass spectrometry, we identified *Nicotiana benthamiana* (*Nb*) transcription factor (TF) NAC2 as a CMV1a-interactor (Extended Data Fig. 1a). NACs constitute a large plant-specific TF family, some of which participate in regulation of within-plant immunity[22]. We searched the *Nb* genome database and found two *NAC2* homologs *NAC2.1* and

87 *NAC2.2* that share 96.7% nucleotide identity and should represent two alleles of one
88 gene from different ancestry of allotetraploid *Nb*. We focused mainly on *NAC2.1*
89 (designated NAC2 hereafter) for further analyses. The CMV1a-NAC2 interaction was
90 verified by co-immunoprecipitation (Co-IP), bimolecular florescence (BiFC), and
91 luciferase complementation imaging (LCI) assay (Extended Data Fig. 1b-d). We
92 evaluated whether *NAC2* affects CMV infection in *NAC2.1/NAC2.2* double-knockout
93 (KO) mutants (*nac2*) which were generated by CRISPR-Cas9 gene editing (Extended
94 Data Fig. 2a) versus (vs) wild-type (WT) plants. CMV infection resulted in severer
95 symptom and higher accumulation of viral RNA and coat protein (CP) in *nac2* than WT
96 plants (Extended Data Fig. 1e-g). Similar results were also obtained in *nac2* vs WT
97 plants infected by GFP-tagged *Potato virus Y* (PVY-GFP, a Potyvirus in the family
98 *Potyviridae*) or GFP-tagged TMV (TMV-GFP) (Extended Data Fig. 1h-m). These data
99 suggest that *NAC2* is essential for plant antiviral defense.

100 **NAC2 mediates AD against aphids via MeSA**

101 By serendipity we noticed that many more apterous green peach aphids colonized on
102 *nac2* than WT leaves. This unexpected discovery led us to examine the role of NAC2
103 in plant attractiveness to aphids. We performed circular-dish and Y-tube olfactometer
104 bioassays, and found that *nac2* plants attracted more aphids (*Myzus persicae*, Sulzer)
105 than WT plants, likely mediated by an airborne signal(s) (Extended Data Fig. 1n, o). To
106 determine which volatile was alterably generated, we used GC-MS assay to identify
107 volatiles emitted by aphid-attacked WT vs *nac2* plants. MeSA was the only constant
108 VOC differentially produced in aphid-attacked WT vs *nac2* plants, and more MeSA

was emitted by WT than *nac2* plants after aphid infestation (Extended Data Fig. 2e-h). Consistently, MeSA is a well-documented major or even the only aphid-inducible VOC in certain plant species[10-13]. To test whether the effect of *NAC2* on plant attractiveness to aphid is attributed to MeSA emission, we measured the emission rate of aerial MeSA from aphid-attacked WT plants by GC-MS and found that aerial MeSA was emitted at approx. 34 ng/h (equivalent to 0.816 μg/day) per aphid-attacked WT plant (Extended Data Fig. 2f). Furthermore, we found that the aerial MeSA concentrations in chambers containing either 0.8 μg MeSA-trapped lanolin paste (MeSA/lanolin) or an aphid-attacked WT plant was similar (Extended Data Fig. 2i, j). Thus, we used 0.8 μg MeSA/lanolin per chamber, which is equal to at approx. 3 nM for the following experiments. After smearing plants with MeSA/lanolin, *nac2* and WT plants showed similar attractiveness to aphids (Extended Data Fig. 1p, q). However, when treated with lanolin alone or lanolin with other volatiles such as 3,3-dimethyl-hexane, *nac2* plants were more attractive to aphids than WT plants (Extended Data Fig. 1r, s). We also kept *nac2* and WT plants under volatile MeSA for 24 hours followed by 2-hour ventilation, and compared how gaseous MeSA would affect plants to attract aphids. Under such conditions, WT plants were more repellent to aphids (Extended Data Fig. 1t, u). However, no obvious difference in aphid repellence was observed between *nac2* plants that were given with and without volatile MeSA followed by ventilation (Extended Data Fig. 1v, w). Further, like that without MeSA treatment, *nac2* remained more attractive to aphids than WT plants after volatile MeSA treatment followed by ventilation (Extended Data Fig. 1x, y).

To decipher reason(s) behind the intriguing phenomenon (Extended Data Fig. 1t-y), we treated *nac2* or WT plants with volatile MeSA for 24 hours followed by ventilation, and then quantified volatized MeSA emitted by MeSA-receiving plants (receivers). WT, but not *nac2* plants emitted higher level of airborne MeSA (Fig. 1a, b). We next compared aphid attractiveness in MeSA-receivers vs mock WT plants after smearing all plants with MeSA/lanolin, but found that they showed no difference in aphid preference (Fig. 1c, d). Moreover, after smearing both *nac2* and WT receivers with MeSA/lanolin, these MeSA-receivers also appeared equally to attract aphids (Fig. 1e, f). We then used aphid-attacked plants as emitters to unravel the role of *NAC2* in plant AD under natural open-air environment (Extended Data Fig. 3a). After infestation by aphid sap-sucking, WT plants constantly emitted VOC MeSA (Fig. 1g, h). Intriguingly, *nac2* receivers released less volatile MeSA, but exhibited higher attractiveness to aphids than WT receivers when emitters were attacked by aphids (Fig. 1i-l). Besides, WT receivers neighboring aphid-attacked emitters were more repellent to aphids than those neighboring mock emitters, while no significant difference in aphid repellence was found between *nac2* receivers neighboring mock- and aphid-attacked emitters (Fig. 1m, n). Furthermore, aphid-feeding in emitters reduced aphid survival in WT but not *nac2* receivers after 24 hours feeding in receivers (Fig. 1o, p). These results suggest that once MeSA is perceived, MeSA biosynthesis in neighboring receiver plants is regulated in a *NAC2*-dependent manner to mediate AD against aphids.

NAC2 activates *SAMT1* transcription

We next set up to dissect the molecular and genetic link between NAC2 and MeSA

153 biosynthesis. As a TF (Extended Data Fig. 3b), NAC2 was found to localize in nucleus
154 (Extended Data Fig. 3c). We then performed RNA-seq and comparative transcriptome
155 analysis in WT and *nac2* plants with or without aphid feeding, and identified numerous
156 potential NAC2-regulated differentially expressed genes (Extended Data Fig. 4 and
157 Supplementary Table 1 and 2), of which *SAMT1* was of particular interest (Extended
158 Data Fig. 4e). *SAMT1* RNA level was lower in *nac2* than WT plants, no matter whether
159 these plants were attacked by aphids or not (Supplementary Table 1 and 2). Knowing
160 that SAMT1 converts SA into MeSA[19], we quantified *SAMT1* transcripts in *nac2*, HA-
161 NAC2-overexpressing, and WT leaf tissues to assess whether NAC2 transcriptionally
162 modulates *SAMT1* expression. Primers used in qRT assays were listed in
163 Supplementary Table 3. *SAMT1* mRNA level was substantially reduced in *nac2* but
164 increased in HA-NAC2 overexpressing plants compared to WT plants (Extended Data
165 Fig. 3d, e). Moreover, Luciferase reporter assay showed that NAC2 enhanced
166 transcription of reporter genes under the control of the *SAMT1* promoter ($SAMT1_{pro}$) *in*
167 *vivo* (Extended Data Fig. 3f). ChIP-qPCR, yeast-one-hybrid, and electrophoretic
168 mobility shift assay (EMSA) all demonstrated that NAC2 bound to the *SAMT1*
169 promoter at the putative NAC TF-binding site[23] and activated reporter gene
170 transcription (Extended Data Fig. 3g-i). Moreover, transient *NAC2* over-expression
171 increased MeSA production in plants (Extended Data Fig. 3j). These results suggest
172 that a NAC2-SAMT1 module involves the regulation of the MeSA biosynthesis in
173 plants.

174 **SA-activated NAC2-SAMT1 module elicits AD**

To investigate if NAC2 affects MeSA production in receivers via activating *SAMT1* transcription, we evaluated *NAC2* and *SAMT1* mRNA levels in *nac2, NahG*, and WT plants with or without airborne volatized MeSA treatment followed by ventilation. Exogenous MeSA dramatically increased *SAMT1* and *NAC2* mRNAs in WT plants, but did not affect *SAMT1* mRNA level in *nac2* plants (Fig. 2a, b). Plants can sense MeSA as a within-plant signal and convert intracellular MeSA into SA to elicit intracellular defense[17,20]. Considering that MeSA treatment did not change much expression of *NAC2* and *SAMT1* as well as aphid repellence in *NahG* plants (Fig. 2a-c), we hypothesized that SA might be the cue to initiate *NAC2* expression. To test this hypothesis, we first examined the effect of aphid attack on *NAC2* expression and found that *NAC2* transcription was upregulated in aphid-attacked plants (Fig. 2d). Then, we examined the effect of aphid attack on SA and MeSA production as well as *SAMT1* expression in WT vs *nac2* plants. In the absence of aphids, lower MeSA accumulated in *nac2* than WT plants (Fig. 2f). Upon aphid infestation, SA level increased in both WT and *nac2* plants to similar extents; however, increases in cellular MeSA and *SAMT1* expression were only found in WT but not *nac2* plants (Fig. 2e-g). Similar results were also found in WT receivers and *nac2* receivers neighboring with aphid-attacked plants (Fig. 2h-j). These results suggest that NAC2 is required for aphid-directed induction or aphid-mediated volatile priming of *SAMT1* expression and MeSA production. Moreover, externally applied SA upregulated *NAC2* and *SAMT1* expression in WT plants, whereas did not significantly alter *SAMT1* mRNA level in *nac2* (Fig. 2k, l). Exogenous SA also induced stronger MeSA volatilization and aphid repellence in WT than *nac2* plants (Fig. 2m-p), and increased the levels of *NAC2* and *SAMT1* transcripts in *SAMT1*-KO (*samt1*) plants (Fig. 2q and Extended Data Fig. 2b, c). In addition, *samt1* plants were more attractive to aphids whilst externally applied SA failed to induce aphid

repellence in *samt1* plants (Fig. 2r-t). Furthermore, volatile MeSA production was compromised in *samt1* plants exposed to aphids-attack (Fig. 3a, b). In further aphid behavior experiments, we uncovered that WT receivers neighboring aphid-attacked WT emitters were more repellent to aphids than those with mock WT emitters, while no significant difference in aphid repellence was found in WT receivers neighboring *nac2* or *samt1* emitters despite whether these emitters were exposed to aphids or not (Fig. 3c-e). These results further confirm the role of MeSA as a PPC signal for interplant AD. Collectively, our data demonstrate that SA can activate *NAC2-SAMT1* transcription to increase MeSA volatilization in both emitter and receiver plants.

As an SA-binding protein, SABP2 can also bind to MeSA and is essential for the conversion of intracellular MeSA into SA[17,20]. Thus, SABP2 may act as an OBP-like receptor that perceives and converts the volatized MeSA generated from emitters into SA to trigger NAC2-mediated aphid resistance in receivers. To test this idea, we first confirmed that SABP2 bound to SA (Fig. 3f), and then examined whether MeSA could influence the specific SABP2 SA-binding activity in competition binding assays (Fig. 3g). We set the SABP2-[^{3}H]SA (50 Ci/mmol) binding capacity in the absence of competitor MeSA as 100%. However, under the same experimental conditions, the binding activity of [^{3}H]SA by SABP2 reduced to approx. 74% and 46% in the presence of 3 nM and 15 nM MeSA, respectively (Fig. 3g). Thus, 3 nM MeSA was sufficient to compete with [^{3}H]SA for binding to SABP2, suggesting that MeSA can bind to SABP2 at physiological concentration. We next generated *SABP2*-KO lines (*sabp2*) and tested aphid repellence in *sabp2* vs WT receivers with volatized MeSA treatment followed by ventilation. Such volatile MeSA treatment increased aphid repellence and SA biosynthesis in WT but not *sabp2* receivers (Fig. 3h-j and Extended Data Fig. 2d). Furthermore, aphid-feeding in WT emitters increased aphid repellence in WT but not

sabp2 receivers (Fig. 3k). In addition, after external applications of SA, no difference in the volatized MeSA amount was found between WT and *sabp2* plants, indicating that SABP2 is not required for MeSA emission (Fig. 3l, m). These results demonstrate that SABP2 is indeed an OBP-like receptor that perceives and converts airborne MeSA into SA to elicit NAC2-mediated aphid repellence in receiver plants.

SAMT1 is required for plant antiviral defense[24]. To test if SAMT1 is a component in NAC2-mediated plant antiviral defense. We knocked-down (KD) *NAC2* in *samt1* to generate *nac2/samt1* double-mutant by *Tobacco rattle virus* (TRV)-based virus-induced gene silencing (VIGS). Like *nac2* mutants, *NAC2*-KD plants (in WT *Nb* background) showed normal growth and were susceptible to CMV and PVY (Extended Data Fig. 1e-j and 5a-e, h-l), suggesting that *NAC2*-KD by VIGS mimics *NAC2*-KO. However, *nac2/samt1* and *samt1* plants showed similar degrees of CMV or PVY infection (Extended Data Fig. 5a-e, h-l). In addition, CMV infection enhanced the intracellular MeSA level in plants (Extended Data Fig. 5f), while *NAC2*-KD, *samt1*, and *nac2*/*samt1* produced similar amount of MeSA, but all lower than WT plants in systemic leaves during virus infection (Extended Data Fig. 5g). Moreover, we investigated whether and how MeSA are responsible for NAC2-mediated plant antiviral defense by treating *nac2*, *sabp2*, *samt1*, and WT plants with external application of either MeSA or SA. Compared to WT, *nac2*, *samt1*, and *sabp2* were more susceptible to CMV and PVY (Fig. 3n, o). However, exogenous MeSA rescued virus hypersusceptibility phenotypes of *nac2* or *samt1* but not *sabp2* plants (Fig. 3n, o), likely due to MeSA conversion into SA in WT, *nac2* and *samt1* but not *sabp2.* On the other hand, external spray of SA rescued virus hypersusceptibility phenotypes of *nac2*, *samt1*, and *sabp2* plants (Fig. 3n, o), consistent with the fact that SA can suppress infection of plants by many viruses including CMV, *Potato virus X* (PVX), and TMV[25].

Taken together, our results demonstrate that SA can trigger the NAC2-SAMT1 module to increase *in vivo* MeSA production by activating the NAC2-driven transcription of *SAMT1*. SA converted from perceived MeSA by SABP2 is the cue to elicit AD against aphids and viruses in receiver plants.

CMV1a destabilizes NAC2 to suppress AD

Aphid-induced PPC and AD may impose some impacts on viral transmission by aphids. To investigate this, we fed CMV-bearing aphids on WT-R/AE, i.e., WT receiver (WT-R) plants neighboring virus-free **a**phid-damaged WT plants as **e**mitters (AE) or WT-R/mE, i.e., WT-R plants adjoining non-aphid damaged WT plants as **m**ock **e**mitters (mE), and analyzed the aphid feeding behaviors on these plants by electrical penetration graph (EPG). EPG showed that number of short intracellular punctures (potential drop, pd) of individual aphids, which is responsible for non-persistent aphid-transmission of CMV, was less in WT-R/AE than WT-R/mE plants (Fig. 4a), suggesting that AD reduced aphids to transmit CMV in WT-R/AE plants. Furthermore, we fed WT-R/AE or WT-R/mE plants with viruliferous aphids for 2 hours, removed all aphids from plants afterwards, and tested viral accumulation in these plants 24 hours later. We found that WT-R/AE plants accumulated less CMV than WT-R/mE plants, evidenced by reduction of viral RNA or CP, respectively (Fig. 4b, c). In addition, fewer viruliferous aphids survived in WT-R/AE than WT-R/mE plants that were fed with viruliferous aphids for 24 hours (Fig. 4d). These results suggest that PPC elicits AD against aphids (including repellent and survival) and reduces their ability to transmit CMV. We also tested the effect of using CMV-carrying aphids attacked plants as emitters (ACE) on AD, and

found that pd number of individual aphids, CMV accumulation, and proportion of living aphids were similar in WT-R/ACE and WT-R/mE plants (Fig. 4e-h). These data suggest that CMV infection can suppress interplant aphid-induced AD. However, the short probing frequency of aphids differs in WT vs CMV-infected plants[26]. By contrast, no difference in short probes frequency is observed in aphid-fed WT vs CMVΔ2b-infected plants[26]. Nevertheless, to assure that the effect of CMV infection on aphid-induced AD was not caused by probing frequency difference between virus-free and viruliferous aphids, we conducted EPG experiments and found that the pd number was lower for virus-free than CMV-carrying aphids, but similar for virus-free and CMVΔ2b-carrying aphids (Fig. 4i), consistent with the previous report[26]. We then fed WT-R/mE, WT-R/AE, WT-R/ACE, and WT-R/ACΔE (WT Receiver with WT plants attacked by **a**phids carrying **C**MV**Δ**2b as **e**mitters) plants with viruliferous aphids for 2 hours, and tested viral accumulation as well as aphid survival in these plants. We found that AD against aphids and viruses was attenuated in WT-Rs that were positioned nearby either ACE or ACΔE (Fig. 4j-l). We next investigated if virus infection affects MeSA production in plants. GC-MS analysis revealed that plants fed with CMV-carrying aphids or CMVΔ2b-carrying aphids emitted less MeSA than plants fed with virus-free aphids (Fig. 4m, n). Taken together, these data suggest that CMV infection can suppress aphid-induced AD for the benefit of aphid survival and virus transmission/infection, likely via a CMV-mediated interference with MeSA production.

The CMV1a-NAC2 interplay (Extended Data Fig. 1a-d) suggests that CMV1a might be involved in CMV-mediated suppression of AD. To test this, we first generated

294 transgenic *Nb* expressing CMV1a (Extended Data Fig. 6a, b) and evaluated the effect
295 of CMV1a on plant attractiveness to aphids and AD. Our circular-dish and Y-tube
296 olfactometer bioassays showed that CMV1a expression caused higher plant
297 attractiveness to aphids (Extended Data Fig. 6c, d). EPG assays revealed that the
298 number of pd of individual aphids was more in CMV1a vs WT plants (Extended Data
299 Fig. 6e). Further, when virus-free aphid-attacked CMV1a plants were used as emitter
300 (1a-AE), AD against aphids and viruses in WT-R was suppressed (Extended Data Fig.
301 6f-h). In addition, WT-R plants nearby non-aphid-attacked WT plants as mock emitters
302 (WT-mE) exhibited higher attractiveness to aphids than WT-Rs adjacent to virus-free
303 aphid-attacked WT plants as emitter (WT-AE), however WT-R plants exhibited similar
304 attractiveness to aphids when non-aphid-attacked or virus-free aphid-attacked
305 transgenic CMV1a plants were used as emitters (1a-mE or 1a-AE) in Y-tube
306 olfactometer bioassays (Extended Data Fig. 6i, j). Moreover, WT-R plants exhibited
307 higher attractiveness to aphids when the emitter was 1a-AE vs WT-AE (Extended Data
308 Fig. 6k). These data imply that CMV1a is involved in CMV-mediated suppression of
309 AD.
310 To understand the importance of CMV1a-NAC2 interaction in CMV-mediated AD
311 suppression, we identified a key amino-acid in CMV1a responsible for its interaction
312 with NAC2. CMV1a protein consists of an N-terminal methyltransferase and a C-
313 terminal ATP-dependent helicase domain (HD). We found that CMV1a HD is
314 responsible for the CMV1a-NAC2 interaction by LCI (Extended Data Fig. 6l). We also
315 modeled the structure of CMV1a-NAC2 complex by AlphaFold-Multimer[27] and

observed that Glycine (G) at position 983 in CMV1a has the nearest physical proximity with NAC2, predicting that this residue might be essential for CMV1a to interact with NAC2 (Extended Data Fig. 6m, n). Indeed, a G983D mutation in CMV1a HD or full-length CMV1a dramatically impaired the CMV1a-NAC2 interaction in Co-IP or BiFC assays (Extended Data Fig. 6o-q).

We next investigated subcellular localization of CMV1a-NAC2 interaction by BiFC and found that CMV1a interacted with NAC2 in both nucleus and cytoplasm (Extended Data Fig. 1c), which is different from NAC2 localization without CMV1a co-expression (Extended Data Fig. 3c), suggesting that CMV1a can relocate some NAC2 from nucleus to cytoplasm. Consistently, CMV1a-MYC, but neither cLUC-MYC nor CMV1a^{G983D}-MYC, partially caused cytoplasmic localization of RFP-NAC2 and less RFP fluorescence in nucleus (Extended Data Fig. 7a). Notably, CMV1a-MYC did not alter RFP nuclear localization, indicating that CMV1a-MYC-directed NAC2 re-localization depends on the NAC2-CMV1a interaction (Extended Data Fig. 7b). Further, we investigated the stability of cytoplasmic NAC2 by using nuclear export signal (NES)-tagged NAC2. We found that NES-NAC2 was localized in cytoplasm and subjected to 26S-proteasome system-mediated degradation than WT NAC2 (Extended Data Fig. 7c, d). Moreover, transient CMV1a expression enhanced NAC2 degradation by the 26S-proteasome system but did not affect RFP stability (Extended Data Fig. 7e-i), while CMV1a^{G983D} failed to cause NAC2 degradation (Extended Data Fig. 7f-i). Further transient expression assays showed that CMV1a but not CMV1a^{G983D} suppressed NAC2-mediated activation of the *SAMT1* promoter (Extended Data Fig. 7j).

In addition, Y-tube olfactometer bioassays and GC-MS analysis in CMV1a^{G983D} or CMV1a transgenic vs WT plants showed that CMV1a^{G983D} impaired CMV1a-mediated plant attractiveness to aphids and suppression of MeSA volatilization (Extended Data Fig. 7k-m). Moreover, when non-aphid-attacked or virus-free aphid-attacked transgenic CMV1a^{G983D} plants were used as emitters (1a^{G983D}-mE or 1a^{G983D}-AE), WT-R plants nearby 1a^{G983D}-mE exhibited higher attractiveness to aphids than WT-R plants adjacent to 1a^{G983D}-AE (Extended Data Fig. 7n). These Y-tube olfactometer bioassays provide additional evidence confirming that the amino acid residue G983 is essential for CMV1a to suppress the interplant AD.

Taken together, our data suggest that CMV1a interferes with AD by affecting subcellular localization and stability of NAC2 via its direct interaction with NAC2 to impair NAC2-drived *SAMT1* transcription and MeSA production.

Some aphid-borne viruses suppress AD

CMV1a with methyltransferase and helicase activity, which forms part of the viral replicase complex, interacts with NAC2 through its HD (Extended Data Fig. 1a-d and 6l-q). We aligned HDs of viral replicases and other HD-containing proteins of multiple plant viruses transmitted by aphids or other vectors. Intriguingly, the HDs from many aphid-transmitted viruses including *Potyvirus, Cucumovirus, Luteovirus*, and *Alfamovirus* contain a conserved glycine at position corresponding to CMV1a G983 (Extended Data Fig. 8, 9a). We further confirmed that PVY infection affected plant MeSA volatilation after aphid attack. We tested the effect of using virus-free aphids-

attacked plants as emitters (AE) on AD against PVY transmission, and found that WT-R/AE plants accumulated less PVY than WT-R/mE plants, evidenced by reduction of viral RNA and CP (Extended Data Fig. 9b, c). Further, GC-MS analysis revealed that plants fed with PVY-carrying aphids emitted less MeSA than plants fed with virus-free aphids (Extended Data Fig. 9d, e). We also tested the effect of using PVY-carrying aphids attacked plants as emitters (APE) on AD, and found that PVY accumulation and proportion of living aphids were similar between WT-R/APE and WT-R/mE plants (Extended Data Fig. 9f-h). Moreover, we showed that two aphid-transmitted viruses CMV and PVY enable to relocate NAC2 from nucleus to cytoplasm (Extended Data Fig. 9i). Similarly, PVY CI, but not CI^{G347D} nor 126KD protein of non-aphid transmitted virus TMV, interacted with NAC2 (Extended Data Fig. 9j, k) and partially impaired nuclear localization of NAC2 (Extended Data Fig. 9l). These results reveal that some aphid-transmitted viruses have evolved to deploy HD-containing proteins as a general strategy to interfere with plant AD.

Discussion

Insect-attacked plants emit VOCs as interplant signals to elicit AD in non-attacked neighboring receiver plants[11,28-30]. However, it is completely unknown how receiver plants perceive VOCs from neighboring stressed “emitter” plants and activate signal transduction to elicit AD[3]. In this study, we reveal molecular genetic mechanism underlying AD against aphids in plants.

Unlike chewing herbivore attacks, phloem-feeding insects such as aphids avoid or suppress jasmonate (JA)-based defense response, instead, they elicit SA response and

increase SA level in attacked plants[31,32]. As outlined in our model (Extended Data Fig. 10a), NAC2 can be activated by upregulated SA level and directly bind to *SAMT1* promoter, activating its transcription (Fig. 2k and Extended Data Fig. 3d-i). SAMT1 then catalyzes SA to form MeSA[19,24]. Consistently, MeSA is a predominant VOC induced by aphid attack in numerous plant species such as bean, chilli, and peach, but it is very low or absent in the VOC emissions induced by beetle attack or artificial wounding[10-13,33]. The OBP-like receptor for perceiving airborne MeSA in receiver plants is yet unknown[3]. SABP2 is thought to be a potential receptor for airborne MeSA because it binds to MeSA[3,17,20]. However, it has been only reported to operate in the same plants exposed to stress (i.e., within-plant signaling)[3]. We now show that SABP2 is an OBP-like receptor for perceiving airborne MeSA from emitter plants and converting MeSA into SA in receiver plants (between-plant signaling) (Fig. 3f-j). Thus, plants may possess an OBP-like receptor-mediated sense system to perceive diverse airborne VOCs[3]. Because MeSA can mediate resistance to many insects including aphids through attracting their predators or parasitoids in multiple plant species[34-38], MeSA-perceived plants are also likely to attract aphid parasitoids or predators via volatile MeSA. MeSA-perceived plants repel aphids and reduce aphid survival fitness (Fig. 1m, o and 4d and Extended Data Fig. 1t, u). Thus, NAC2-SAMT1-mediated airborne PPC represents a multifunctional strategy to prevent aphid epidemic infestation.

Arabidopsis SA methyltransferase *BSMT1* is strongly induced by JA and biotic stress-induced MeSA production, therefore severely compromised in JA pathway mutants

while SA signaling mutants such as *npr1* or *pad4* do not show compromised MeSA emission[39]. This is different to the regulation of *NbSAMT1* by SA described in this study. Nevertheless, our finding of *SAMT1* induction by exogenous SA, intracellular SA upon aphid attack, or aphid-mediated volatile priming via NAC2 in *N. benthamiana* (Fig. 2a-l and Extended Data Fig. 3d-j) is consistent with that *SAMT1* can be induced by SA or insect feeding in *Atropa belladonna* and rice[40,41] as well as in *N. alata* and *N. sylvestris*[42]. It is possible that diverse species may have evolved distinctive mechanisms to regulate *BSMT1* vs *SAMT1* expression. MeSA biosynthesis can also respond to environmental biotic and abiotic stresses in a plant species-specific manner.

MeSA has been extensively studied as a long-distance mobile signal and shown to be involved in the induction of SAR to viruses and aphids, and herbivore-induced within plants[11,12,14,17]. In this study, NAC2-SAMT1 module participates in intra/interplant defense against CMV, PVY, and TMV (Extended Data Fig. 1e-m and 5a-e, h-l). MeSA-mediated AD induces aphid antixenosis and suppresses virus transmission by aphids in neighboring receiver plants (Fig. 4a-d). Hence, the NAC2-SAMT1 module is important not only for plant intra/intercellular antiviral defense but also for AD against aphids and viral transmission among plants. Therefore, we have now unraveled a completely novel role of MeSA in PPC and AD, which is in a NAC2-dependent manner.

Elucidation of the molecular insight into AD against aphids and viruses raises an intriguing question on whether and how virus counteracts AD and affects aphid survival in receiver plants. In some cases, virus infection benefits its insect vector in virus-infected plants. For examples, TYLCCNV-encoded βC1 protein suppresses JA pathway

or reduces terpene synthase and alters glucosinolate profiles to increase whitefly *Bemisia tabaci* attraction and performance in virus-infected plants[43,44]. CMV 2b protein targets plant JA pathway or alters emission of VOC (not MeSA) to induce attractiveness of virus-infected plants to aphids[45,46]. In addition, CMV1a, which influences viral replicase complex assembly and viral systemic movement, prevents CMV 2b-induced anti-aphid resistance (antibiosis), likely via limiting CMV 2b-Argonaute1 interaction[47]. Further, CMV 2a stimulates feeding deterrence against aphids[48]. Moreover, NIa-Pro encoded by PVY or TuMV increases ethylene production and inhibits callose accumulation to benefit insects in virus-infected plants[49,50]. However, there is no report about mechanism underlying pathogen-induced regulation of MeSA-mediated plant AD[2]. We now reveal that some aphid-transmitted viruses can suppress MeSA emission in aphid-attacked plants to impair AD against virus infection and aphid infestation in adjacent plants (Fig. 4e-n and Extended Data Fig. 9b-h). This is achieved by the action of the helicase domain-containing protein that suppresses AD through its interaction with NAC2 to partially change the subcellular localization of NAC2 from nucleus to cytoplasm, and to promote the NAC2 degradation via the 26S proteasome to block *SAMT1* transcription and subsequent MeSA biosynthesis (Extended Data Fig. 10b). Therefore, some aphid-transmitted viruses have evolved to use helicase domain-containing proteins as a common means to suppress NAC2 transcription function and counteract AD in plants. These findings further suggest that not only viruses can utilize aphids as vector for transmission, but also aphids can in turn exploit viruses to facilitate their surviving and thriving in plants. This unexpected countermeasure reveals an

447 undefined ecological and co-evolutionary mutualism between aphids and aphid-
448 transmissible viruses (Extended Data Fig. 10).

449 # References

450 1. van Emden, H. & Harrington, R. Aphids as Crop Pests Second Edition Preface
451 to the Second Edition. *Aphids as Crop Pests, 2nd Edition*, Xxiii-Xxiv (2017).

452 2. Karban, R. Plant Communication. *Annual Review of Ecology, Evolution, and*
453 *Systematics,* **52**, 1-24 (2021).

454 3. Loreto, F. & D'Auria, S. How do plants sense volatiles sent by other plants?
455 *Trends in Plant Science* **27**, 29-38 (2022).

456 4. Shulaev, V., Silverman, P. & Raskin, I. Airborne signalling by methyl salicylate
457 in plant pathogen resistance. *Nature* **386**, 738-738 (1997).

458 5. Wenig, M. *et al.* Systemic acquired resistance networks amplify airborne
459 defense cues. *Nature Communications* **10**, 3813 (2019).

460 6. Pickett, J.A. & Khan, Z.R. Plant volatile-mediated signalling and its application
461 in agriculture: successes and challenges. *New Phytologist* **212**, 856-870 (2016).

462 7. Sugimoto, K. *et al.* Identification of a tomato UDP-arabinosyltransferase for
463 airborne volatile reception. *Nature Communications* **14,** 677 (2023).

464 8. Bleecker, A.B. & Schaller, G.E. The mechanism of ethylene perception. *Plant*
465 *Physiology* **111**, 653-660 (1996).

466 9. Fereres, A. & Moreno, A. Behavioural aspects influencing plant virus
467 transmission by homopteran insects. *Virus Research* **141**, 158-168 (2009).

468 10. Babikova, Z. *et al.* Underground signals carried through common mycelial
469 networks warn neighbouring plants of aphid attack. *Ecology Letters* **16**, 835-
470 843 (2013).

471 11. Moreira, X., Nell, C.S., Katsanis, A., Rasmann, S. & Mooney, K.A. Herbivore
472 specificity and the chemical basis of plant-plant communication in Baccharis
473 salicifolia (Asteraceae). *New Phytologist* **220**, 703-713 (2018).

474 12. Staudt, M. *et al.* Volatile organic compound emissions induced by the aphid
475 Myzus persicae differ among resistant and susceptible peach cultivars and a
476 wild relative. *Tree Physiology* **30**, 1320-1334 (2010).

477 13. Saad, K.A., Mohamad Roff, M.N., Hallett, R.H. & Idris, A.B. Aphid-induced
478 Defences in Chilli Affect Preferences of the Whitefly, Bemisia tabaci

(Hemiptera: Aleyrodidae). *Scientific Report* **5**, 13697 (2015).

14. Dong, Y.J. & Hwang, S.Y. Cucumber Plants Baited with Methyl Salicylate Accelerates Scymnus (Pullus) sodalis (Coleoptera: Coccinellidae) Visiting to Reduce Cotton Aphid (Hemiptera: Aphididae) Infestation. *Journal of Economic Entomology* **110**, 2092-2099 (2017).

15. Mallinger, R.E., Hogg, D.B. & Gratton, C. Methyl Salicylate Attracts Natural Enemies and Reduces Populations of Soybean Aphids (Hemiptera: Aphididae) in Soybean Agroecosystems. *Journal of Economic Entomology* **104**, 115-124 (2011).

16. Ninkovic, V., Glinwood, R., Unlu, A.G., Ganji, S. & Unelius, C.R. Effects of Methyl Salicylate on Host Plant Acceptance and Feeding by the Aphid Rhopalosiphum padi. *Frontiers in Plant Science* **12**, 710268 (2021).

17. Park, S.W. Methyl salicylate is a critical mobile signal for plant systemic acquired resistance. *Science* **321**, 342-342 (2008).

18. Vlot, A.C., Dempsey, D.A. & Klessig, D.F. Salicylic Acid, a Multifaceted Hormone to Combat Disease. *Annual Review of Phytopathology* **47**, 177-206 (2009).

19. Dudareva, N., Raguso, R.A., Wang, J.H., Ross, E.J. & Pichersky, E. Floral scent production in Clarkia breweri - III. Enzymatic synthesis and emission of benzenoid esters. *Plant Physiology* **116**, 599-604 (1998).

20. Forouhar, F. *et al.* Structural and biochemical studies identify tobacco SABP2 as a methyl salicylate esterase and implicate it in plant innate immunity. *Proceedings of the National Academy of Sciences of the United States of America* **102**, 1773-1778 (2005).

21. Wang, Y.J. *et al.* A calmodulin-binding transcription factor links calcium signaling to antiviral RNAi defense in plants. *Cell Host & Microbe* **29**, 1393-1406 (2021).

22. Olsen, A.N., Ernst, H.A., Lo Leggio, L. & Skriver, K. NAC transcription factors: structurally distinct, functionally diverse. *Trends in Plant Science* **10**, 79-87 (2005).

23. De Clercq, I. *et al.* The Membrane-Bound NAC Transcription Factor ANAC013 Functions in Mitochondrial Retrograde Regulation of the Oxidative Stress Response in Arabidopsis. *Plant Cell* **25**, 3472-3490 (2013).

24. Zhu, F. *et al.* Salicylic acid and jasmonic acid are essential for systemic resistance against tobacco mosaic virus in Nicotiana benthamiana. *Molecular Plant-Microbe Interactions* **27**, 567-77 (2014).

25. Naylor, M., Murphy, A.M., Berry, J.O. & Carr, J.P. Salicylic acid can induce resistance to plant virus movement. *Molecular Plant-Microbe Interactions* **11**, 860-868 (1998).

26. Guo, H.J. *et al.* Aphid-borne Viral Spread Is Enhanced by Virus-induced Accumulation of Plant Reactive Oxygen Species. *Plant Physiology* **179**, 143-155 (2019).

27. Evans, R. *et al.* Protein complex prediction with AlphaFold-Multimer. *bioRxiv* https://doi.org/10.1101/2021.10.04.463034 (2021).

28. Arimura, G. *et al.* Herbivory-induced volatiles elicit defence genes in lima bean leaves. *Nature* **406**, 512-515 (2000).

29. Engelberth, J., Alborn, H.T., Schmelz, E.A. & Tumlinson, J.H. Airborne signals prime plants against insect herbivore attack. *Proceedings of the National Academy of Sciences of the United States of America* **101**, 1781-1785 (2004).

30. Karban, R., Yang, L.H. & Edwards, K.F. Volatile communication between plants that affects herbivory: a meta-analysis. *Ecology Letters* **17**, 44-52 (2014).

31. Donovan, M.P., Nabity, P.D. & DeLucia, E.H. Salicylic acid-mediated reductions in yield in Nicotiana attenuata challenged by aphid herbivory. *Arthropod-Plant Interactions* **7**, 45-52 (2013).

32. Cao, H.H., Liu, H.R., Zhang, Z.F. & Liu, T.X. The green peach aphid Myzus persicae perform better on pre-infested Chinese cabbage Brassica pekinensis by enhancing host plant nutritional quality. *Scientific Report* **6**, 21954 (2016).

33. Blande, J.D., Korjus, M. & Holopainen, J.K. Foliar methyl salicylate emissions indicate prolonged aphid infestation on silver birch and black alder. *Tree Physiology* **30**, 404-416 (2010).

34. van Poecke, R.M.P. & Dicke, M. Indirect defence of plants against herbivores: Using Arabidopsis thaliana as a model plant. *Plant Biology* **6**, 387-401 (2004).

35. James, D.G. Field evaluation of herbivore-induced plant volatiles as attractants for beneficial insects: Methyl salicylate and the green lacewing, Chrysopa nigricornis. *Journal of Chemical Ecology* **29**, 1601-1609 (2003).

36. Woods, J.L., James, D.G., Lee, J.C. & Gent, D.H. Evaluation of airborne methyl salicylate for improved conservation biological control of two-spotted spider mite and hop aphid in Oregon hop yards. *Experimental and Applied Acarology* **55**, 401-416 (2011).

37. Rowen, E., Gutensohn, M., Dudareva, N. & Kaplan, I. Carnivore Attractant or Plant Elicitor? Multifunctional Roles of Methyl Salicylate Lures in Tomato

Defense. *Journal of Chemical Ecology* **43**, 573-585 (2017).

38. Liu, J. *et al.* Herbivore-Induced Rice Volatiles Attract and Affect the Predation Ability of the Wolf Spiders, Pirata subpiraticus and Pardosa pseudoannulata. *Insects* **13**, 90 (2022).

39. Attaran, E., Zeier, T.E., Griebel, T. & Zeier, J. Methyl salicylate production and jasmonate signaling are not essential for systemic acquired resistance in Arabidopsis. *Plant Cell* **21**, 954-71 (2009).

40. Kwon, S. *et al.* Biotic and abiotic stresses induce AbSAMT1, encoding S-adenosyl-L-methionine: salicylic acid carboxyl methyltransferase, in Atropa belladonna. *Plant Biotechnology* **26**, 207-215 (2009).

41. Xu, R., Song, F. & Zheng, Z. OsBISAMT1, a gene encoding S-adenosyl-L-methionine: salicylic acid carboxyl methyltransferase, is differentially expressed in rice defense responses. *Molecular Biology Reports* **33**, 223-31 (2006).

42. Hippauf, F. *et al.* Enzymatic, expression and structural divergences among carboxyl O-methyltransferases after gene duplication and speciation in Nicotiana. *Plant Molecular Biology* **72**, 311-330 (2010).

43. Li, R. *et al.* Virulence Factors of Geminivirus Interact with MYC2 to Subvert Plant Resistance and Promote Vector Performance. *Plant Cell* **26**, 4991-5008 (2014).

44. Zhao, P.Z. *et al.* Viruses mobilize plant immunity to deter nonvector insect herbivores. *Science Advances* **5,** eaav9801 (2019).

45. Tungadi, T. *et al.* Cucumber mosaic virus and its 2b protein alter emission of host volatile organic compounds but not aphid vector settling in tobacco. *Virology Journal* **14**, 91 (2017).

46. Wu, D.W. *et al.* Viral effector protein manipulates host hormone signaling to attract insect vectors. *Cell Research* **27**, 402-415 (2017).

47. Westwood, J.H. *et al.* A trio of viral proteins tunes aphid-plant interactions in Arabidopsis thaliana. *PLoS One* **8**, e83066 (2013).

48. Rhee, S.J., Watt, L.G., Bravo, A.C., Murphy, A.M. & Carr, J.P. Effects of the cucumber mosaic virus 2a protein on aphid-plant interactions inArabidopsis thaliana. *Molecular Plant Pathology* **21**, 1248-1254 (2020).

49. Casteel, C.L. *et al.* The NIa-Pro protein of Turnip mosaic virus improves growth and reproduction of the aphid vector, Myzus persicae (green peach aphid). *Plant Journal* **77**, 653-663 (2014).

50. Bak, A., Cheung, A.L., Yang, C.L., Whitham, S.A. & Casteel, C.L. A viral protease relocalizes in the presence of the vector to promote vector performance. *Nature Communications* **8**, 14493 (2017).

Figure legends

Fig. 1 | *NAC2* regulates MeSA production to mediate PPC-induced aphid resistance.

a, b, GC-MS analysis. WT, but not *nac2* plants emitted higher level of airborne MeSA after MeSA treatment followed by ventilation**. c, d,** After smearing plants with MeSA-containing lanolin, WT and volatile MeSA-treated WT plants exhibited similar attractiveness to aphids in circular-dish **(c)** or Y-tube olfactometer **(d)** bioassays**. e, f,** Once smearing plants with MeSA-containing lanolin, volatile MeSA-treated WT and *nac2* plants exhibited similar attractiveness to aphids in circular-dish **(e)** or Y-tube olfactometer **(f)** bioassays**. g-j,** GC-MS analysis. Aphid sap-sucking caused the attacked WT emitter plants to volatilize MeSA **(g, h)**. When aphid-attacked WT plants were used as emitters (AE), their WT receivers (WT-R) volatilize more MeSA than *nac2* receivers (*nac2*-R) **(i, j)**. **k, l,** *nac2*-R (AE) plants exhibited higher attractiveness to aphids than WT-R (AE) plants in circular-dish **(k)** or Y-tube olfactometer **(l)** bioassays. **m, n,** WT-R (AE) plants were more repelled by aphids than those neighboring mock emitter plants **(m)**, while no significant difference in aphid repellence between *nac2* receivers neighboring mock- and aphid-attacked emitter plants **(n)** in Y-tube olfactometer bioassays. **o, p,** Proportion of living aphids in WT-R **(o)** or *nac2*-R **(p)** plants with aphid-attacked WT plants as emitters (AE) or non-aphid-attacked WT plants as mock emitters (mE). Numerals shown inside each bar present number of choice-making aphids. **b, h, j,** Two-sided Student's *t*-test, n=3 biologically independent samples. **o, p,** One-way ANOVA with least significant difference (LSD), n=4 biologically independent samples; letters A-B represent statistically different groups ($P < 0.05$). Data are shown as mean ± s.d.; n.s., no statistical significance. **c-f, k-n,** χ^2 test (df = 1). All P values are shown in figure. Experiments were repeated at least three times with similar results.

Fig. 2 | NAC2 is required for SA-directed enhancement of MeSA volatilization.

a, b, *NAC2* (or its deletion mutant) or *SAMT1* mRNA levels in WT, *nac2*, and *NahG* plants with or without volatile MeSA treatment. **c,** Volatile MeSA treatment induced aphid repellence in WT, but not *NahG* plants in Y-tube olfactometer bioassays. **d,** *NAC2* expression was enhanced in aphid-attacked WT plants. **e-g,** Free SA **(e)**, MeSA **(f)**, and *SAMT1* expression **(g)** in WT or *nac2* plants upon aphid attacks. **h-j,** Free SA **(h)**, MeSA **(i),** and *SAMT1* expression **(j)** in WT or *nac2* receivers neighboring aphid-attacked WT emitters or mock WT emitters. **k, l,** *NAC2* or *SAMT1* expression in *nac2* and WT plants with or without SA treatment. **m, n,** GC-MS analysis of volatized MeSA in WT or *nac2* plants treated with SA for 24 hours. **o, p,** SA treatment induced aphid repellence in WT **(o)**, but not *nac2* **(p)** plants in Y-tube olfactometer bioassays. **q,** *NAC2* or *SAMT1* expression in *samt1* plants with or without SA treatment. **r,** *samt1* plants exhibited higher attractiveness to aphids than WT plants in Y-tube olfactometer bioassays. **s, t,** SA treatment induced aphid repellence in WT **(s)**, but not *samt1* **(t)** plants in Y-tube olfactometer bioassays. **a, b, d, g, j-l, n, q,** Two-sided Student's *t*-test. **e, f, h, i,** One-way ANOVA with Tukey's multiple comparisons test; letters A-C represent statistically different groups (P <0.05). **a, b, d-h, j-l, n, q,** n=3 biologically independent samples. **i**, n=4 biologically independent samples. Data are shown as mean ± s.d.; n.s., no statistical significance. **c, o, p, r-t,** χ^2 test (df = 1). P values are shown in **a-d, g, j-l, n-t**; P values for **e, f, h, i** are shown in the Source Data. Experiments were repeated at least three times with similar results.

Fig.3 | The conversion between MeSA and SA is required for NAC2-mediated AD against aphids and plant defense against viruses.

a, b, Volatile MeSA production was compromised in *samt1* plants exposed to aphids-attack by GC-MS analysis. **c-e,** WT receivers neighboring aphid-attacked WT emitters were more repellent to aphids than those with mock WT emitters **(c)**, while no significant difference in aphid repellence in WT receivers neighboring *nac2* **(d)** or *samt1* **(e)** emitters exposed to aphids or not in Y-tube olfactometer bioassays. **f,** SA-binding activity of purified SABP2 protein. **g,** SA competition binding assays with 0,

3, 15 nM MeSA. Binding activity of [^{3}H]SA to SABP2 in the presence of 3 nM or 15 nM MeSA were calculated against the baselevel. **h,** *sabp2* showed no abnormal developmental phenotypes. **i,** Volatile MeSA treatment induced aphid repellence in WT plants, but not in *sabp2* plants in Y-tube olfactometer bioassays. **j,** Volatile MeSA treatment increased free SA amount in WT, but not *sabp2* plants. **k,** WT receivers with non-aphid-attacked WT plants as mock emitters (WT-mE) exhibited higher attractiveness than those with virus-free aphid-attacked WT plants as emitters (WT-AE), but not for *sabp2* receivers in Y-tube olfactometer bioassays. **l, m,** GC-MS assays. No difference in the volatized MeSA amount was seen between WT and *sabp2* plants after SA treatment. **n, o,** MeSA treatment rescued virus hypersusceptibility phenotypes of *nac2* or *samt1* but not *sabp2* plants, whilst SA treatment rescued virus hypersusceptibility phenotypes of *nac2*, *samt1* and *sabp2* plants. **b, g, j, m-o,** Two-sided Student's *t*-test. **b, f, m-o**, n=3 biologically independent samples. **g, j,** n=4 biologically independent samples. Data are shown as mean ± s.d.; n.s., no statistical significance. **c-e, i, k,** χ^2 test (df = 1). All P values are shown in figure. Experiments were repeated at least three times with similar results.

Fig. 4 | CMV1a suppresses AD.

a, EPG analysis showed the pd number in aphid feeding was less in WT receivers (WT-R) with virus-free aphid-attacked WT plants as emitters (AE) than WT receivers with non-aphid-attacked WT plants as mock emitters (mE) when receivers were fed with CMV-carrying aphids. n=21 individual aphids. **b-d,** CMV RNA **(b)**, CP **(c)** or proportion of living aphids **(d)** in WT-R (mE) and WT-R (AE) plants. **e,** The pd number was similar between WT-R (mE) and WT-R plants with CMV-carrying aphids-attacked plants as emitter (ACE) when these receivers were fed with CMV-carrying aphids. n=20 individual aphids. **f-h,** CMV RNA **(f),** CP **(g)** or proportion of living aphids **(h)** is similar between WT-R (mE) and WT-R (ACE) plants. **i,** The pd number of virus-free aphids was lower than that of CMV-carrying aphids, but similar to that of CMVΔ2b-carrying aphids. n=19 individual aphids. **j-l,** CMV RNA **(j),** CP **(k)** or proportion of living aphids **(l)** in WT-R plants with mE, AE, ACE, or CMVΔ2b-carrying aphid-

attacked WT plants as emitters (ACΔE). **m**, **n**, GC-MS analysis of volatized MeSA in WT plants fed with virus-free aphids, CMV-carrying aphids, or CMVΔ2b-carrying aphids for 3 days. **a, b, e, f, i, j, n,** Two-sided Student's *t*-test. **d, h,** One-way ANOVA with LSD. **l**, One-way ANOVA with Tukey's multiple comparisons test; letters A-B represent statistically different groups ($P < 0.05$). **b, d, f, h, j, l, n,** n=3 biologically independent samples. Data are shown as mean ± s.d.; n.s., no statistical significance. *P* values are shown in **a, b, d-f, h-j, n**; *P* values for **l** are shown in the Source Data. In box plots (**a**, **e**, **i**), the centre line represents the median, box edges delimit bottom and top quartiles and whiskers show the highest and lowest data points. Experiments were repeated at least three times with similar results.

Methods

Plant Materials and Growth Conditions

Nicotiana benthamiana (*Nb*) was used as wild-type (WT) plant. *NahG* lines were transgenic *Nb* plants expressing bacterial *NahG* which encodes SA-degrading enzyme salicylate hydroxylase[51]. Transgenic CMV*1a*, CMV*1a*^{G983D} lines are *Nb* lines overexpressing CMV*1a* or CMV*1a*^{G983D} with C-terminal fusion to a MYC tag. The *nac2*, *samt1*, and *sabp2* were *NbNAC2.1/2.2*, *NbSAMT1*, and *NbSABP2*-edited KO mutant *Nb* lines, respectively. All seeds were surface-sterilized and cultivated on MS medium (Murashige and Skoog medium, Sigma-Aldrich), grown at 26℃ with a 16 h/8 h light/dark photoperiod. 10-day-old seedlings were then planted in soil and grown with the same photoperiod.

Generation of Transgenic Plants

The MYC-tagged full-length CMV*1a* and CMV*1a*^{G983D} genes under the CaMV 35S promoter were cloned into pCambia1300-based binary vector via the ligation-independent cloning strategy. All constructs were verified by DNA sequencing and transformed into *Agrobacterium* GV2260. To generate transgenic plants, leaf discs were

plated on MS medium in 100 mm petri dish (704001, NEST Biotechnology) with 0.1 mg/mL NAA (N8010, Solarbio), 1.0 mg/mL 6-BA (IB0100, Solarbio), 0.2 mg/mL Timentin and 0.025 mg/mL Hygromycin B (400052, Merck Millipore) for callus, shoot, and root regeneration. Western blot assays were used to select the T2 generation transgenic lines of *35S:CMV1a-MYC* and *35S:CMV1a*^{G983D}*-MYC* plants, and selected transgenic plants were then used for aphid attraction bioassays and GC-MS analysis. The Cas9-edited knockout lines were generated as described[52]. Briefly, the fragment containing single sgRNA (NAC2_LacZ/AtU3d-sgRNA, SABP2_LacZ/AtU3d-sgRNA) or two sgRNAs (SAMT1_LacZ/AtU3d-sgRNA1-At3b-sgRNA2) were cloned into pYLCRISPR/Cas9-DH to generate pYLCRISPR/Cas9-DH-NAC2, pYLCRISPR/Cas9-DH-SABP2, and pYLCRISPR/Cas9-DH-SAMT1. The sgRNA sequence is listed in Supplementary Table 3. The editing target site of transgenic plant DNA sequence was characterized by PCR sequencing to select homozygous transgenic lines. PCR amplification was conducted using 2×T5 Super PCR Mix (TSE005, Beijing Tsingke Biotech). Progenies of homozygous *nac2*, *sabp2*, and *samt1* lines showed no developmental phenotype.

MeSA supplement treatment – Lanolin smear assay

0.8 μg pure MeSA chemical (M6752, Sigma-Aldrich) was dissolved in lanolin paste (S5106, Selleck). Plants for MeSA supplement treatment were smeared with MeSA-containing lanolin on the stems or leaf vein. MeSA-containing lanolin would release quantitative volatile MeSA continuously and constantly[53,54].

MeSA supplement treatment – Airborne assay

0.8 μg pure MeSA was dissolved in lanolin paste. Lanolin containing 0.8 μg MeSA was then smeared onto the surface of filter paper and the filter paper was placed in a 2 L

volume gas tight glass chamber. Plants for airborne MeSA supplement treatment were placed in these chambers separately to perceive volatile MeSA (each chamber contains one plant) for 24 hours, and then transferred from chambers to open-air area for ventilation for 2 hours before further experiments as described[55].

Exogeneous SA supply treatment

Solutions of 50 μM SA (S5922, Sigma-Aldrich) were used for plant treatments. 4-week-old seedlings were cultured in pots in a greenhouse and sprayed with the SA solutions.

Aphid choice bioassay: Y-tube olfactometer assay

Wingless *M. persicae* aphids were isolated from *Nb* plants and starved for 2 hours before testing. Plants grown in soil for 4 weeks were used. The experimental procedure and equipment were used as described[46]. For pair-wise comparison of aphid attractiveness, plants in different groups were separately placed into two chambers, which were connected by the two arms of a glass Y-tube. The glass Y-tube was 1.0 cm in inner diameter and 6 cm in arm length. A humidified continuous air flow purified by activated charcoal flowed through the chambers at 200 mL/min, then flowed into the arms of the Y-tube.

In each experiment, an individual aphid was placed at the end of the Y-tube stem. Aphids walked upwind toward the arms and made its choice. Once the aphid entered one arm and walked up to 3 cm away from the Y-junction, their choice would be marked. To avoid any unknown asymmetry in the setup, the plant-containing chambers were switched after every 10 tests, and the Y-tube and plants were replaced after 20 tests. The used Y-tubes were cleaned by ethanol and ddH_2O before reuse. The same number

of aphids were used for each group in each experiment. All experiments were independently repeated at least 3 times.

Aphid choice bioassay: Petri disc assay

Choice test for *M. persicae* was performed with detached leaves from 4 to 5-week-old *Nb* in plastic petri dishes (15 cm diameter) following a previously described procedure[56]. Two leaves with similar leaf position and size from experimental group plants and control group plants were detached and placed in petri dishes, with their petioles inserted in moistened cotton swabs. Twenty wingless adult aphids were released at the midpoint between pairs of leaves, and the aphids on each leaf were counted at 24 hours after their release in the petri dishes. The same number of aphids were used for each group in each experiment. All experiments were independently repeated at least three times.

Interplant communication assays

Experimental plants were served as “emitters” or “receivers” respectively. The emitter and receiver plants were placed on two trays at a distance of 30 cm from each other in an open-air experimental set-up for interplant communication assays. Each emitter was fed with fifty virus-free or viruliferous *M. persicae* aphids or no aphids, then the emitters and receivers were incubated in same cage made by gauze. After 3 days, the receiver plants were taken out for further experiments. Viruliferous *M. persicae* aphids were obtained from aphids which were fed on CMV, CMVΔ2b, or PVY-GFP-infected plants for 1 hour before the pre-acquisition starvation period (2 hours).

Aphid survival and virus-transmission analysis

To measure the effect of plant airborne defense on aphid fitness in neighboring receiver

plants, the experimental group receiver plants and mock receiver plants were fed with the same number of wingless adult *M. persicae*. After 24 hours, numbers of alive aphids on each host plant were counted. To measure the influence of airborne defense on aphid-mediated virus-transmission in neighbor receiver plants, the experimental group receiver plants and control receiver plants were fed with the same number of viruliferous adult aphids (carrying CMV or PVY) for 2 hours as described[57], then aphids were removed, 24 hours later, aphid-sucked leaves were taken to measure viral infection. All experiments were conducted at least three times.

EPG analysis of aphid feeding behavior

Giga-8 EPG amplifier (Wageningen University, Wageningen, Netherlands) was used to study feeding behavior of *M. persicae* on plants as described[58]. The amplifier with eight channels simultaneously recorded eight individual aphids on separate plants for 2 hours in accordance with the inoculation access period (IAP) in viral transmission experiment. The EPG waveforms of short intracellular punctures (potential drop, pd) were analyzed during 2 hours of aphid feeding with the software "Stylet + a".

Measurement of plant endogenous free SA amount

Free SA was extracted and measured as described[59]. Briefly, 0.2 g leave tissue was homogenized in 1 mL of ethyl acetate containing 10 ng of SA-d6, and vortexed for 10 min followed by centrifuging at 18000g at 4 °C for 20 min. Supernatants were collected and evaporated to dry by a vacuum concentrator at 30 °C. 200 μL of MeOH: H_2O (70:30, v/v) was added to resuspend the residues by centrifuging at 18000g for 10 min. The collection of supernatants was analyzed by a high-performance liquid chromatography-

tandem mass spectrometry system (QTRAP 4500, AB Sciex).

Measurement of plant endogenous MeSA

MeSA was extracted and measured by Suzhou Michy Biomedical Technology Co., Ltd. Briefly, frozen leaf tissues (150 mg) was homogenized with 200 μL of extraction buffer (water/1-propanol/HCl = 1:2:0.005). The homogenate was added 500 μL of methylene chloride and shaken thoroughly, then centrifuged at 18800g for phase separation. Aliquots of the supernatants were separated by a gas chromatography (GC) system.

Volatile MeSA measurement by GC-MS analysis

VOCs emitted by plants were collected by a static-headspace sampling device with a solid-phase microextraction (SPME) fibre (PDMS/DVB, 65 μm) coated with polydimethylsiloxane/divinylbenzene (57345-U, Supelco) as described[13]. Each sample was enclosed in a 1.5-L glass container for 120 min, then the SPME fibre was extended into the headspace to collect volatiles for 30 min. After collection of volatile substances, the SPME fibre was inserted directly into a thermal desorption gas chromatograph-mass spectrometer (Thermo Fisher Scientific, Bermen, Germany). The volatiles bound to the fibre were desorbed for 2 min. A Thermo Scientific Trace 1300 gas chromatograph equipped with a Thermo Scientific Q-Exactive Orbitrap mass spectrometer (GC-Orbitrap-MS, Thermo Scientific, Bremen, Germany) was used for HRMS quantitative analysis. The split-splitless injection port was held at 250°C for desorpting volatiles in split mode at a split ratio of 1:10. The oven temperature program was set as: 60 °C held for 2 min, then increased to 280°C at 20°C/min and held for 2 min.

Mass Spectrometry Analysis

Protein extracts were immunoprecipitated by MYC-Trap beads (M20012L, Abmart)

and the mixture was incubated at 4℃ for 3 hours. The precipitated samples were washed 5 times with Co-IP buffer, and immunoprecipites were then separated by 10% SDS-PAGE. The gel was silver stained and gel-embedded protein samples were digested and LC-MS/MS analyzed.

Yeast One Hybrid (Y1H) Assay

The full-length cDNA sequence of *NAC2* was fused in frame with the GAL4 activation domain in pGADT7-Rec2 (Clontech). The fusion construct was co-transformed with the reporter vector (pHIS2-cis/promoter of *SAMT1*) into Y187 yeast cells (Clontech). The empty vector pGADT7-Rec2 and the pHIS2-cis/35S promoter were co-transformed as the negative controls. Co-transformed yeast strain Y187 were spotted on selective media (minus (-) His, Leu and Trp) contained 0.5, 1, or 2 mM 3-AT. Images were taken after 3 days incubation at 28℃. All experiments were repeated at least three times.

Bimolecular fluorescence complementation (BiFC) and firefly luciferase complementation imaging (LCI) assays

BiFC and LCI assays were conducted as described[60]. For BiFC assay, the full-length cDNA sequences of *NAC2*, CMV*1a*, CMV$1a^{G983D}$, PVY*CI*, PVYCI^{G347D}, and TMV*126KD* were cloned into the binary cYFP or nYFP vector by ligation-independent cloning technique. Primer pairs for making these constructs were made by Beijing Tsingke Biotech Co., Ltd. and are listed in Supplementary Table 3. These gene sequences were PCR-amplified by M5 Magic High-Fidelity DNA Polymerase (MF740, Mei5Bio) from plant cDNA or virus vector. The Mut Express II Fast Mutagenesis Kit V2 (C214-01, Vazyme) was used to construct mutants. PCR products were purified by HiPure Gel Pure DNA Mini Kit (D2111-02, Magen, China). The YFP fluorescence

signal for each combination was detected by an inverted confocal microscope (Leica SP8) at 48 hpi. Confocal images were analyzed with Leica LAS X (3.3). Anti-GFP (ab290, Abcam) or anti-Rabbit（HA1001, HUABIO) antibodies were used at a 1:3000 dilution for immunoblot analysis. For LCI assays, the full-length cDNA sequences of CMV*1a*, CMV*1a-H*, CMV*1a-M*, and *NAC2* were cloned into nLUC vector and cLUC vector by ligation-independent cloning assay. The luciferase substrate (luciferin) was smeared onto the surface of leaves and the luciferase activity was captured with a PlantView100 assay system (BLT PHOTON TECHNOLOGY). All experiments were independently repeated at least three times.

Co-immunoprecipitation (Co-IP) Assay

The constructs were transiently co-expressed with indicated combinations in *Nb* leaves. At 48 hpi, the leaves were taken for protein extraction. Protein extracts were immunoprecipitated by RFP-Trap beads (rtma, ChromoTek) in Co-IP buffer [50 mM Tris-HCl, pH 7.5, 150 mM NaCl, 10% glycerol, 0.5 mM EDTA, 0.5% NP-40, 5 mM DTT, 1 mM PMSF and protease inhibitor cocktail (Roche)]. The mixture was incubated for 3 hours at 4℃. The immunoprecipites were then denatured by 2×protein loading buffer contains β-mercaptoethanol (JS0150, Hong Kong JSENB International Trading Co., Ltd) and separated in a 10% SDS-PAGE gel (M00664, GenScript) followed by immunoblot analysis. Anti-MYC (M20002M, Abmart), anti-Mouse (AS003, ABclonal), anti-RFP (5f8-100, ChromoTek), or anti-Rat (AS028, ABclonal) antibodies were used at a 1:3000 dilution for immunoblot analysis. StarSignal Chemiluminescent Assay Kit (E171-01, GenStar) was used for signal detection. All experiments were repeated three times and generated similar results.

RNA-seq Analysis

RNAs extracted from 5-week-old WT and *nac2* plants (without any treatment) were used for RNA-seq analysis. To examine the expression profiles of the WT and *nac2* plants in response to aphids-attack, RNAs extracted from 3-week-old WT and *nac2* plants (2 days post aphid-infestation) were used for RNA-seq analysis. RNA-seq was performed by Biomarker Technologies (www.biomarker.com.cn). Raw data were processed by Illumina NovaSeq 6000 sequencer (2 × 150 bp read length) and aligned to *Nb* reference genome (https://solgenomics.net/). Differential expression genes (DEGs) were identified according to the transcripts per million reads (TPM) (log_2(foldchange) ≥ 1 or ≤ -1 and $P \leq 0.05$). Furthermore, Gene Ontology (GO, http://www.geneontology.org) and Kyoto Encyclopedia of Genes and Genomes (KEGG, http://www.genome.jp/kegg/) were performed to identify DEGs that were significantly enriched in GO terms and KEGG pathways.

Electrophoretic Mobility Shift Assay (EMSA)

GST and GST-NAC2 proteins were purified by Glutathione Sepharose 4B (GE Healthcare) affinity chromatography and eluted by 10 mM GSH followed by size exclusion chromatography (Superdex 200 10/300, GE Healthcare). Oligonucleotide probes were labeled with the biotin by RUIBIO Technology Company. DdH2O was purified by Milli Q (Merck) water purification system. Chemiluminescent EMSA Kit (GS009, Beyotime) was used for EMSA. The detailed protocol was described[21]. EMSA experiments were repeated at least three times.

Quantitative Real-Time PCR (qRT-PCR)

Total RNA was extracted with TransZol reagent (TransGen Biotech) and retained in 1.5

mL sterile centrifugal tube (HRK-150-TP, Beijing Huaruikang Technology Co., Ltd.). Then 5 μg of RNA was reverse-transcribed into cDNA with TransScript One-Step gDNA Removal and cDNA Synthesis SuperMix (AT311-02, TransGen Biotech). qRT-PCR was performed with Hieff® qPCR SYBR Green Master Mix (11201ES08, YEASEN). Data was normalized to *ACTIN* expression by the cycle threshold (CT) $2^{-\Delta\Delta^{CT}}$ method as described[61] and analyzed by Prism9 software (Graphpad). All experiments were repeated at least three times. Primers used for qRT-PCR are listed in Supplementary Table 3. Data are represented as mean ± s.d.

Virus infection and analysis of viral RNA and protein

For testing the effect of *NAC2* on virus infection, *nac2* and *Nb* plants were grown in soil for 3-4 weeks and infected with CMV[62], PVY-GFP[63], or TMV-GFP through agro-infiltration. Viral symptoms were photographed at 6 days post-inoculation (dpi) for CMV and TMV-GFP, 7 dpi for PVY-GFP. For performing virus infection in silenced plants, 20-day-old WT or *samt1* plants were first agro-infiltrated with TRV-*NAC2* or TRV, and the upper leaves were then infected with CMV or PVY-GFP at 14 days after VIGS treatment. Viral symptoms were photographically recorded at 7 dpi for CMV and PVY-GFP. Anti-CMV (CMV21-A, Alpha diagnostic international), anti-PVY (POTY11-A, Alpha diagnostic international), anti-TMV (TMV11-A, Alpha diagnostic international), anti-Rabbit (HA1001, HUABIO), or anti-Goat (BE0103, EASYBIO) antibodies were used at a 1:3000 dilution for immunoblot analysis.

For testing whether and how MeSA is responsible for NAC2-mediated plant antiviral defense. *nac2*, *samt1*, *sabp2*, and *Nb* plants were grown in soil for 3-4 weeks, and plants were sprayed with control or solutions of 500 μM SA or MeSA a daily for 3 days prior to infection with CMV or PVY-GFP as described[64,65]. Systemic leaves were taken for viral infection analysis at 6 or 7 dpi.

907 **Chromatin immunoprecipitation-quantitative (ChIP-qPCR)**

908 ChIP-qPCR was performed following the published protocol with minor
909 modifications[66]. *Nb* leaves over-expressing HA-NAC2 or HA-nLUC were collected
910 and chromatin isolated from 2 g of frozen leaf tissue was sonicated with a Bioruptor
911 sonicator for 6 min. SimpleChIP® Plus Kit (9005S, CST) was used to perform the
912 experiment. Enrichment of promoter DNA was measured using the % input method by
913 qRT-PCR analysis as described[67]. Amplification of *ACTIN2* promoter sequence served
914 as the negative control. Primers for the ChIP-qPCR assays are listed in Supplementary
915 Table 3. ChIP-qPCR experiments were repeated for three times and all showed similar
916 results.

917 **Semi-*In Vivo* and *In Vivo* Protein Degradation**

918 For chemical treatments, MG132 (C2211, Sigma), cycloheximide (CHX) (HY-12320,
919 MedChemExpress), and ATP (IA1310, Solarbio) were used. MG132 and CHX were
920 dissolved in DMSO and used at a concentration of 100 μM. ATP was used at the
921 concentration of 10 mM.

922 For semi-*in vivo* protein degradation analysis, *Nb* leaves over-expressing CMV1a-
923 MYC, CMV1a^{G983D}-MYC, RFP-NAC2, or cLUC-MYC were collected after 2 days
924 post-infiltration. The proteins were respectively extracted with extraction buffer (50
925 mM Tris-MES pH 8.0, 0.5 M sucrose, 1 mM $MgCl_2$, 10 mM EDTA, 5 mM DTT,
926 protease inhibitor cocktail) as described[68]. For analysis of NAC2 degradation by the
927 26S proteasome, the plant extract harboring RFP-NAC2 was mixed with chemicals
928 containing CHX, then the extract was split equally into two tubes, one tube was added
929 into ATP, the other was added equal volume of extraction buffer. Two tubes were
930 incubated in the Eppendorf Thermomixer at 25˚C, and extracts were respectively
931 removed from two tubes as samples at different time points. For analysis of CMV1a-

mediated promotion of NAC2 protein degradation via the ubiquitin-proteasome pathway, the RFP-NAC2 extract was mixed with CMV1a-MYC, CMV1a^{G983D}-MYC, or cLUC-MYC extracts in a ratio of 1:1 before incubation. ATP and CHX together with MG132 or DMSO were added to the prepared leaf extracts. The samples were collected at different time points.

For *in vivo* analysis of NAC2 or NES-NAC2 protein degradation by the 26S proteasome, RFP-NAC2 or RFP-NES-NAC2 were transiently expressed in *Nb* leaves for 60 h. Then, the agro-inoculated leaves were treatment with MG132 or an equal volume of DMSO control solution for 12 hours before sampling. For *in vivo* analysis of NAC2 protein degradation promoted by CMV1a, RFP-NAC2 were co-expressed with CMV1a-MYC, CMV1a^{G983D}-MYC, or cLUC-MYC respectively for 60 hours before MG132 treatment for 12 hours.

SA-MeSA competition binding assay

[^{3}H]SA binding of SABP2 was performed as described with modifications[20,69]. The GST-SABP2 proteins were expressed in *E. coli* and purified. The size exclusion columns were prepared by adding 0.13 g of sephadex G-25 (GE healthcare) to QIAGEN shredder columns. The columns were preequilibrated with reaction buffer (50 mM Tris-HCl, 150 mM NaCl, pH 7.5) containing 0.1% Tween-20 overnight at 4˚C, and excess buffer was removed by spinning at 735 g for 2 min. The GST-SABP2 proteins were respectively incubated with 10 nM, 20 nM, 50 nM, and 100 nM [^{3}H]SA (50 Ci/mmol) in reaction buffer on ice for 1 hour, and then loaded to the columns and centrifuged immediately as above. The flow-through was collected and the radioactivity was measured with 2 ml Ultima Gold™ AB Cocktails (PerkinElmer) by a scintillation counter (MicroBeta2; PerkinElmer). For SA-MeSA competition binding experiments, the GST-SABP2 proteins were incubated with 50 nM [^{3}H]SA in the presence of 0 nM,

3 nM or 15 nM MeSA on ice for 1 hour. Binding activity of [^{3}H]SA (50 Ci/mmol) by SABP2 in the absence of competitor MeSA was set to 100%, and binding activity of [^{3}H]SA by SABP2 with 3 nM or 15 nM MeSA was calculated along with comparison. GraphPad Prism 9.0 was used to construct nonlinear binding model of Michaelis-Menten equation.

Alignment of helicase domain

Sequences of viral helicase domain-containing proteins were retrieved from Uniprot (https://www.uniprot.org/). Multiple sequence alignments of proteins were done in Jalview using Mafft (L-INS-i method) (http://www.jalview.org/About).

Statistical analysis

Statistical significance was determined by two-sided Student's *t*-test or one-way ANOVA with Tukey's multiple comparisons test for multiple groups (≥3) of data. For aphid attraction bioassays, data were statistically analyzed using the χ^2 test. For analyzing aphid survival portion in two groups, data were statistically analyzed using one-way ANOVA with least significant difference (LSD). Statistical analysis was performed with GraphPad Prism 9.0 or IBM SPSS Statistics 26. Detailed statistical analyses are explained in figure legends, and *P* values are indicated in figures or Source Data. The chromatographic (TIC) data of each sample was exported by The Xcalibur 4.1 software. Graphics were drawn by GraphPad Prism 9.0 software. For quantification analysis of blots, the intensities of bands were quantified with ImageJ software.

Reporting summary

Further information on research design is available in the Nature Research Reporting Summary linked to this article.

Data availability

All data and materials needed to replicate the work are available. *NAC2.1* (Niben101Scf01481g02006), *NAC2.2* (Niben101Scf07152g04032), *SAMT1* (Niben101Scf05122g00005), and *SABP2* (Niben101Scf00034g00012) from *Nicotiana benthamiana* genome database (https://solgenomics.net/). RNA-seq raw data have been deposited in National Center for Biotechnology Information (NCBI) under Bioproject PRJNA851626 (WT), PRJNA851854 (*nac2*), PRJNA955195 (WT-aphid), and PRJNA955395 (*nac2*-aphid). Original data in graphs are shown in Source data files and uncropped gel and immunoblotting images are shown in Supplementary Figure 1. Source data are provided with this paper.

References

51. Ying, X.B. *et al.* RNA-Dependent RNA Polymerase 1 from Nicotiana tabacum Suppresses RNA Silencing and Enhances Viral Infection in Nicotiana benthamiana. *Plant Cell* **22**, 1358-1372 (2010).

52. Ma, X. *et al.* A Robust CRISPR/Cas9 System for Convenient, High-Efficiency Multiplex Genome Editing in Monocot and Dicot Plants. *Molecular Plant* **8**, 1274-84 (2015).

53. Kessler, A. & Baldwin, I.T. Defensive function of herbivore-induced plant volatile emissions in nature. *Science* **291**, 2141-2144 (2001).

54. Kost, C. & Heil, M. Herbivore-induced plant volatiles induce an indirect defence in neighbouring plants. *Journal of Ecology* **94**, 619-628 (2006).

55. Ozawa, R., Arimura, G., Takabayashi, J., Shimoda, T. & Nishioka, T. Involvement of jasmonate- and salicylate-related signaling pathways for the production of specific herbivore-induced volatiles in plants. *Plant and Cell Physiology* **41**, 391-398 (2000).

56. Feng, H. *et al.* Acylsugars protect Nicotiana benthamiana against insect herbivory and desiccation. *Plant Molecular Biology* **1-18**(2021).

57. Fernandez-Calvino, L., Lopez-Abella, D., Lopez-Moya, J.J. & Fereres, A. Comparison of Potato virus Y and Plum Pox Virus transmission by two aphid species in relation to their probing behavior. *Phytoparasitica* **34**, 315-324 (2006).

58. Verdier, M., Chesnais, Q., Pirolles, E., Blanc, S. & Drucker, M. The cauliflower mosaic virus transmission helper protein P2 modifies directly the probing behavior of the aphid vector Myzus persicae to facilitate transmission. *PLoS Pathogens* **19**, e1011161 (2023).

59. Xu, H.X. *et al.* A salivary effector enables whitefly to feed on host plants by eliciting salicylic acid-signaling pathway. *Proceedings of the National Academy of Sciences of the United States of America* **116**, 490-495 (2019).

60. Wang, Y. *et al.* Geminiviral V2 Protein Suppresses Transcriptional Gene Silencing through Interaction with AGO4. *Journal of Virology* **93**, e01675-18 (2019).

61. Livak, K.J. & Schmittgen, T.D. Analysis of relative gene expression data using real-time quantitative PCR and the 2(-Delta Delta C(T)) Method. *Methods* **25**, 402-8 (2001).

62. Wang, X.B. *et al.* The 21-nucleotide, but not 22-nucleotide, viral secondary small interfering RNAs direct potent antiviral defense by two cooperative argonautes in Arabidopsis thaliana. *Plant Cell* **23**, 1625-38 (2011).

63. Geng, C. *et al.* Tobacco vein banding mosaic virus 6K2 Protein Hijacks NbPsbO1 for Virus Replication. *Scientific Report* **7**, 43455 (2017).

64. Mayers, C.N., Lee, K.C., Moore, C.A., Wong, S.M. & Carr, J.P. Salicylic acid-induced resistance to Cucumber mosaic virus in squash and Arabidopsis thaliana: Contrasting mechanisms of induction and antiviral action. *Molecular Plant-Microbe Interactions* **18**, 428-434 (2005).

65. Bi, H.H., Zeng, R.S., Su, L.M., An, M. & Luo, S.M. Rice allelopathy induced by methyl jasmonate and methyl salicylate. *Journal of chemical ecology* **33**, 1089-103 (2007).

66. Saleh, A., Alvarez-Venegas, R. & Avramova, Z. An efficient chromatin immunoprecipitation (ChIP) protocol for studying histone modifications in Arabidopsis plants. *Nature Protocol* **3**, 1018-25 (2008).

67. Yamaguchi, N. *et al.* PROTOCOLS: Chromatin Immunoprecipitation from Arabidopsis Tissues. *Arabidopsis Book* **12**, e0170 (2014).

68. Liu, L. *et al.* An efficient system to detect protein ubiquitination by agroinfiltration in Nicotiana benthamiana. *Plant Journal* **61**, 893-903 (2010).

69. Slaymaker, D.H. *et al.* The tobacco salicylic acid-binding protein 3 (SABP3) is the.chloroplast carbonic anhydrase, which exhibits antioxidant activity and plays a role in the hypersensitive defense response. *Proceedings of the National Academy of Sciences of the United States of America* **99**, 11640-11645 (2002).

Acknowledgments

We thank Le Kang for his constructive suggestions, Xiangdong Li and Xianbing Wang for providing PVY-GFP and CMV (CMV-Fny and CMVΔ2b, the latter is a CMV *2b* gene deletion mutant) infectious clones respectively, Pingzhi Zhao and Jian Ye for assistance in measurement of SA amount, De Li for her assistance in the radiolabeling experiments. We thank Facility Center of Metabolomics and Lipidomics of China National Center for Protein Sciences for GC-MS analysis. This work was supported in part by National Key R&D Program of China (2022YFD1400800 and 2021YFD1400400), the National Natural Science Foundation of China (32130086, 31920103013, and 31872636), the Young Elite Scientists Sponsorship Program by CAST (2022QNRC001), and Shuimu Tsinghua Scholar Program.

Author contributions

Y.L. conceived the research. Q.G., Y.J.W., and Y.L. designed all experiments. Q.G. and Y.J.W. performed all aphid choice bioassays, SA-MeSA competition binding experiments, semi-*in vivo* and *in vivo* protein degradation experiments, ChIP-qPCR, EMSA, GC-MS analysis experiments, virus infection and analysis of viral RNA and protein experiments, and aphid survival as well as virus-transmission analysis. Y.J.W., L.H. and F.H. performed BiFC, Y1H and LCI experiments. Y.J.W., D.Z., Y.W., and X.W. generate transgenic plants. Q.G., L.L., and F.C. performed EPG analysis. Y.J.W.,

H.M., and H.D. performed Mass Spectrometry analysis. Q.G., Y.J.W., Y.H., and Y.L. analyzed data, wrote paper with input from all authors.

Competing interests

The authors declare no competing interests.

Extended data are available for this paper

Extended Data Figs. 1-10

Additional information

Supplementary Table 1-3

Extended data figures

Extended Data Fig. 1 | NAC2 interacts with CMV1a and is required for plant antiviral defense and MeSA mediated aphid repellence.

a, Representative LC-MS/MS spectrum of peptides in NAC2 protein. A peptide (**AGIAQDAFVLCR**) is shown. **b-d,** Confirmation of the CMV1a-NAC2 interaction. In Co-immunoprecipitation (Co-IP) assay (**b**), cLUC-MYC or CMV1a-MYC was co-expressed with RFP-NAC2 in *Nb* leaves and analyzed 2 days post-infiltration (dpi). Both Bimolecular fluorescence complementation (BiFC) **(c)** and firefly luciferase complementation imaging (LCI) assays **(d)** further confirmed CMV1a-NAC2 interaction in *Nb* leaves. Scale bar = 25 μm. **e-g,** Viral symptoms in WT and *nac2* plants infected with CMV at 6 dpi **(e)**, and the relative accumulation of CMV RNA **(f)** or CP **(g)** in CMV-infected systemic leaves of WT or *nac2* plants. **h-j,** Viral symptoms in WT and *nac2* plants infected with PVY-GFP at 7 dpi **(h)**, and the accumulation of PVY RNA **(i)** or CP **(j)** in PVY-GFP infected systemic leaves of WT or *nac2* plants. **k-m,** Viral symptoms in WT and *nac2* plants infected with TMV-GFP at 6 dpi **(k)**, and the relative accumulation of TMV RNA **(l)** or CP **(m)** in TMV-GFP infected systemic leaves of WT or *nac2* plants. **n, o,** *nac2* plants exhibited higher attractiveness to aphids

than WT plants in circular-dish **(n)** or Y-tube olfactometer bioassays **(o)**. Numerals shown inside each bar present number of choice-making aphids. **p, q,** *nac2* plants smeared with MeSA containing lanolin exhibited similar attractiveness to aphids with WT plants under same treatment in circular-dish bioassay **(p)** or Y-tube olfactometer bioassays **(q)**. **r, s,** *nac2* plants smeared with lanolin alone or with 3,3-dimethyl-hexane containing lanolin exhibited higher attractiveness to aphids than WT plants under same treatment in circular-dish **(r)** or Y-tube olfactometer bioassays **(s)**. **t, u,** Volatile MeSA treatment caused WT plants more repellent to aphids in circular-dish bioassay **(t)** or Y-tube olfactometer bioassays **(u). v, w,** No significant difference in aphid repellence between *nac2* plants with and without volatile MeSA treatment in circular-dish **(v)** or Y-tube olfactometer **(w)** bioassays**. x, y,** After volatile MeSA treatment followed by ventilation, *nac2* plants showed higher attractiveness to aphids than WT plants in circular-dish **(x)** or Y-tube olfactometer **(y)** bioassays**. f, i, l,** Two-sided Student's *t*-test, n=3 biologically independent samples. Data are shown as mean ± s.d.. **n-y**, χ^2 test (df = 1). All *P* values are shown in figure. Experiments were repeated at least three times with similar results.

Extended Data Fig. 2 | GC-MS analysis of VOCs emitted from WT and *nac2* plants.

a-d, Direct sequencing of PCR product containing targeted sites in CRISPR/Cas9-edited knockout *nac2*, *samt1*, and *sabp2* homozygous plants. The rectangular area indicates the start positions at or from which the mutations occurred. It is worth mentioning that there is only one *SAMT1* or *SABP2* copy in *N.benthamiana* genome although *Nb* is allotetraploid. **e,** GC-MS analysis of VOCs emitted from WT and *nac2* plants after 48 h aphid feeding. Wet weight per plant was 1.10 g on average. Identifications based on retention indices and GC-MS: (1) oxalic acid, allyl hexyl ester; (2) bicyclo[3.1.0]hex-2-ene, 2-methyl-5-(1-methylethyl)-; (3) benzene, 1,2,3-trimethyl-; (4) 6-methyl heptanoate; (5) butyl pyruvate; (6) benzene, 1,2,3,5-tetramethyl-; (7) methyl salicylate; (8) tridecane, 4-methyl-; (9) 3,3-dimethyl-hexane; (10) Cyclohexasiloxane, dodecamethyl-; (11) bicyclo[3.1.1]heptane, 6,6-dimethyl-3-

methylene-; (12) heptane, 2,2,3,3,5,6,6-heptamethyl-; (13) heptane, 2,3,6-trimethyl-; (14) 2,2,4-Trimethyl-1,3-pentanediol diisobutyrate; (15) phenol, 2,6-bis(1,1-dimethylethyl)-4-(1-methylpropyl)-. **f,** The mean amounts of volatile MeSA collected from the aphid-attacked plants in GC-MS analysis. **g, h,** Mass spectrum of putative MeSA produced by plants **(g)** and the authentic MeSA standard **(h)**. **i, j,** Comparison of the aerial MeSA concentrations in chambers containing either MeSA dissolved lanolin paste or aphid attacked WT plants by GC-MS analysis. Experiments were repeated at least three times with similar results.

Extended Data Fig. 3 | NAC2 binds to *SAMT1* promoter to activate its transcription.

a, Emitter and receiver plants were placed on two trays at a distance of 30 cm from each other in an interplant communication assay set-up in open-air environment. Each emitter was fed with fifty virus-free or viruliferous *M. persicae* aphids or no aphids before the emitters and receivers were incubated in same cage (100 cm × 70 cm × 70 cm) made by gauze. After 3 days, the receiver plants were taken out for further experiments. **b,** NbNAC2 and AtNAC2 share similar conserved motifs. **c,** RFP-tagged NAC2 showed nuclear localization, scale bar = 20 μm. **d, e,** qRT-PCR quantification of relative *SAMT1* mRNA levels in *nac2* and WT plants **(d)** or leaves transiently over-expressing HA-NAC2 and HA-nLUC **(e)**. **f,** Transient expression assays. *NAC2* activates luciferase reporter gene transcription under the control of the *SAMT1* promoter (*SAMT1pro*) in *Nb* leaves. Photograph was taken at 48 hours post-infiltration (hpi). **g,** *In planta* ChIP-qPCR. HA-NAC2, but not HA-nLUC, specifically binds to the *SAMT1* promoter DNA. Chromatin from plants expressing HA-nLUC or HA-NAC2 were immunoprecipitated and amplified with promoter-specific primers. **h,** Yeast one-hybrid assay. Yeast cells were co-transformed with an effector vector containing the *SAMT1pro* cloned into pHis2 vector and a prey vector encoding NAC2 cloned into pGADT7. **i,** *In vitro* EMSA. Hot probe is the biotin-labeled NAC2-binding motif DNA of *SAMT1pro*, cold probe or cold mutant probe is the unlabeled NAC2-binding motif DNA of *SAMT1pro* or its mutant DNA. **j,** Transient over-expression of *NAC2* increases MeSA

production in plants, the samples were collected at 48 hpi. **d, e, g, j,** Two-sided Student's *t*-test, *n*=3 biologically independent samples. Data are shown as mean ± s.d.; n.s., no statistical significance. All *P* values are shown in figure. Experiments were repeated at least three times with similar results.

Extended Data Fig. 4 | RNA-seq transcriptome analysis of WT and *nac2* plants. **a,** Comparison of WT and *nac2* plants (without any treatment) RNA-seq sequences on the reference genome. The Phred quality score Q20 (99% base call accuracy) and Q30 (99.9% base call accuracy) were used to measure the quality of RNA sequencing. **b,** Hierarchical clustered heat map of 90 differential expressed genes (DEGs, 24-up genes and 66-down genes) based on the $\log_2$ (fold change) in transcript levels of WT and *nac2* plants. **c,** Kyoto Encyclopedia of Genes and Genomes (KEGG) pathway analysis of 90 DEGs in (**b**), the module with the most enriched genes is "metabolism" (green color, marked by red font). **d,** Gene ontology (GO) analysis of 90 DEGs in (**b**), the "biological process" module (green color) with the most enriched genes is "metabolism process" (marked by red font). **e,** Phylogenetic analysis of SAMT1 proteins from various plant species. NtSAMT1, *Nicotiana tabacum* SAMT1 (GenBank ID: FJ015052); SlSAMT1, *Solanum lycopersicum* SAMT1 (GenBank ID: NM_001247880); AtBSMT1, *Arabidopsis thaliana* BSMT1 (Tair ID: AT3G11480); AtGAMT1 (Tair ID: AT4G26420); AtIAMT1 (Tair ID: AT5G55250). **f,** Comparison of WT (aphid) and *nac2* (aphid) plants (under aphid attack) RNA-seq sequences on the reference genome. **g,** Hierarchical clustered heat map of 157 DEGs (100-up genes and 57-down genes) based on the $\log_2$(fold change) in transcript levels of WT (aphid) and *nac2* (aphid) plants. **h,** KEGG pathway analysis of 157 DEGs in (**g**), the module with the most enriched genes is "metabolism" (green color, marked by red font). **i,** GO analysis of 157 DEGs in (**g**), the "biological process" module (green color) with the most enriched genes is "metabolism process" (marked by red font). All DEGs were identified according to the transcripts per million reads (TPM) ($\log_2$ (foldchange) ≥ 1 or ≤ -1 and $P \leq 0.05$).

Extended Data Fig. 5 | *NAC2* regulates *SAMT1* to fulfill anti-CMV and PVY function.

a-e, Analysis of antiviral role of *NAC2* and *SAMT1* during CMV infection in *nac2*, *samt1*, or *nac2*/*samt1* double mutants. Viral symptoms **(a)**, relative *NAC2* mRNA levels in *NAC2*-silenced WT **(b)** or *NAC2*-silenced *samt1* plants **(c)**, the accumulation of CMV RNA **(d)** or CP protein **(e),** and plant endogenous MeSA amount **(f, g)** of WT, *nac2*, *samt1*, or *nac2*/*samt1* double mutant plants infected with CMV. **h-l,** Analysis of antiviral role of *NAC2* and *SAMT1* during PVY-GFP infection in *nac2*, *samt1*, or *nac2*/*samt1* double mutants. Viral symptom **(h)**, relative *NAC2* mRNA levels in *NAC2*-silenced WT **(i)** or *NAC2*-silenced *samt1* plants **(j)**, PVY RNA accumulation **(k)** or PVY CP **(l)** of *nac2*, *samt1*, or *nac2*/*samt1* double mutant plants infected with PVY-GFP. Plants in panels **(a** and **h)** were photographed at 7 days post-inoculation (dpi). *NAC2*-knockdown (KD) was triggered by VIGS vector TRV-*NAC2* to mimic *nac2* mutant while TRV was used as negative control in these experiments. **b-d, f, g, i-k,** Two-sided Student's *t*-test, n=3 biologically independent samples. Data are shown as mean ± s.d.. All *P* values are shown in figure. Experiments were repeated at least three times with similar results.

Extended Data Fig. 6 | CMV1a suppresses MeSA-mediated AD, and CMV1a^{G983D} impairs its interaction with NAC2.

a, Transgenic CMV*1a-MYC* or CMV*1a*^{G983D}*-MYC* expression *Nb* plant showed normal growth and development. **b,** CMV1a-MYC and CMV1a^{G983D}-MYC were detected in transgenic plants by western blot. Rubisco was used as loading control. **c, d,** Transgenic CMV1a plants exhibited higher attractiveness to aphids than WT plants in circular-dish **(c)** or Y-tube olfactometer **(d)** bioassays**. e,** EPG analysis showed that the number of pd of individual aphids was more in CMV1a plants than WT plants. n=19 individual aphids. **f-h,** Accumulation of CMV RNA **(f)**, CP **(g)** or proportion of living aphids **(h)** in CMV-carrying aphid-attacked leaves of WT receivers (WT-R) with non-aphid-attacked WT plants as mock emitters (WT-mE), virus-free aphid-attacked WT plants as emitters (WT-AE), non-aphid-attacked transgenic CMV1a plants as mock emitters (1a-mE), or virus-free aphid-attacked transgenic CMV1a plants as emitters (1a-AE). **i, j,** WT-R (WT-mE) plants exhibited higher attractiveness than WT-R (WT-AE) plants **(i)**,

but WT-R plants showed similar attractiveness to aphids when non-aphid-attacked or virus-free aphid-attacked CMV1a plants were used as emitters (1a-mE or 1a-AE) **(j)** in Y-tube olfactometer bioassays. **k,** WT-R plants nearby virus-free aphid-attacked CMV1a plants as emitters (1a-AE) exhibited higher attractiveness to WT-R plants close to virus-free aphid-attacked WT plants as emitters (WT-AE). **l,** LCI assay to show that CMV1a helicase domain (1a-H), but not methyltransferase domain (1a-M), interacts with NAC2. **m,** AlphaFold-Multimer predicted CMV1a-H-NAC2 interacting complex (parameters: "MMseqs2" and "AlphaFold2-Multimer-v2" pattern). Colours are given based on AlphaFold-Multimer-calculated prediction score: pLDDT. Protein structures with scores over 90 are represented in blue (very high confidence of prediction); scores between 70 and 90 in light blue (high confidence); scores between 50 and 70 in yellow (low), and anything below 50 in orange (very low confidence of prediction). **n,** Red and blue indicate the CMV1a-H and NAC2, respectively. The stick model represents the potential interacting site between 1a-H and NAC2, this region is predicted with a high confidence score. **o,** Co-IP assay to show that G983D mutation in CMV1a helicase domain impairs the 1a helicase domain-NAC2 interaction. **p, q,** Co-IP assay **(p)** and BiFC assay **(q)** to show that CMV1a^{G983D} failed to interact with NAC2 in *Nb.* Scale bar = 25 μm. **e, f,** Two-sided Student's *t*-test. **h,** One-way ANOVA with Tukey's multiple comparisons test; letters A-B represent statistically different groups ($P < 0.05$). **f, h,** n=3 biologically independent samples. Data are shown as mean ± s.d.; n.s., no statistical significance. **c, d, i-k,** χ^2 test (df = 1). *P* values are shown in **c-f, i-k**; adjusted *P* values for **h** are shown in the Source Data. In box plot **(e)**, the centre line represents the median, box edges delimit bottom and top quartiles and whiskers show the highest and lowest data points. Experiments were repeated at least three times with similar results.

Extended Data Fig. 7 | CMV1a re-localizes and degrades NAC2 by 26S-proteasome system, and CMV1a^{G983D} possesses a weakened aphid repellence.

a, CMV1a but not CMV1a^{G983D} partially changed NAC2 localization from nucleus to cytoplasm. **b,** CMV1a did not alter subcellular localization of RFP. **c, d,** Nuclear exit signal-tagged RFP-NAC2 (NES-NAC2) changed NAC2 localization to cytoplasm **(c)**

and enhanced 26S-proteasome system-dependent degradation **(d)**. Scale bar = 25 μm in panels (**a-c**). **e,** Immunoblot assay of RFP protein levels. **f,** Immunoblots to show cLUC-MYC, CMV1a-MYC, and CMV1a^{G983D}-MYC protein levels with anti-MYC antibody. **g,** *In vivo* assay showing effects of MG132 and the CMV1a-NAC2 interaction on NAC2 protein stability. 100 μM MG132 or an equal volume of DMSO (negative control) was infiltrated into leaves transiently co-expressing RFP-NAC2 with CMV1a-MYC, CMV1a^{G983D}-MYC, or cLUC-MYC for 12 hours before harvesting. **h,** Semi-*in vivo* assay to show that NAC2 protein stability is ATP-dependent. NAC2 protein levels were analyzed with anti-RFP antibody at different times following 100 μM CHX treatment in the presence or absence of 10 mM ATP. **i,** Semi-*in vivo* assay to show that MG132 inhibits CMV1a-promoted NAC2 degradation. RFP-NAC2, cLUC-MYC, CMV1a-MYC, or CMV1a^{G983D}-MYC was transiently expressed in *Nb* leaves and extracted respectively. NAC2 degradation was performed as below: The RFP-NAC2 protein extract was mixed with the cLUC-MYC, CMV1a-MYC, or CMV1a^{G983D}-MYC extracts in a 1:1 volume of 100 μM CHX and 10 mM ATP, in the presence of 100 μM MG132 or an equal volume of control DMSO. **j,** Effect of CMV1a on expression of luciferase reporter gene driven by the *SAMT1* promoter (*SAMT1pro*). Transient expression assays in *Nb* leaves to show that CMV1a but not CMV1a^{G983D} suppressed NAC2-mediated activation of the *SAMT1* promoter. Photographs were taken at 48 hpi. **k,** Transgenic plants expressing CMV*1a*, but not CMV*1a*^{G983D}, exhibited higher attractiveness to aphids than WT plants in Y-tube olfactometer bioassays**. l, m,** GC-MS analysis to show that transgenic plants expressing CMV*1a*, but not CMV*1a*^{G983D}, emitted less volatized MeSA than WT plants once they were fed with virus-free aphids for 3 days. **n,** WT-R (WT-mE) plants exhibited higher attractiveness than WT-R (WT-AE) plants, WT-R plants showed similar attractiveness to aphids when non-aphid-attacked or virus-free aphid-attacked CMV*1a*-expressinig plants were used as emitters (1a-mE or 1a-AE), whilst WT-R (1a^{G983D}-mE) plants exhibited higher attractiveness than WT-R (1a^{G983D}-AE) plants in Y-tube olfactometer bioassays. **m**, Two-sided Student's *t*-test, *n*=3 biologically independent samples. Data are shown as mean ± s.d.;

n.s., no statistical significance. **k**, **n**, χ^2 test (df = 1). All *P* values are shown in figure. Experiments were repeated at least three times with similar results.

Extended Data Fig. 8 | Alignment of helicase domain from aphid and non-aphid transmitted viruses.

BCMNV, *Bean common mosaic necrosis virus* (Uniprot ID: Q65399); BYMV, *Bean yellow mosaic virus* (Uniprot ID: P17765); MDMV, *Maize dwarf mosaic virus* (Uniprot ID: J7II85); PPV, *Plum pox potyvirus* (Uniprot ID: P13529); PRSV, *Papaya ringspot virus* (Uniprot ID: A0A1L2DBW1); PVY, *Potato virus Y* (Uniprot ID: A0A5J6BDG4); PeMV, *Pepper mottle virus* (Uniprot ID: Q01500); PVMV, *Pepper veinal mottle virus* (Uniprot ID: A0A6J4A295); SCMV, *Sugarcane mosaic virus* (Uniprot ID: A0A0K0Y0R3); SMV, *Soybean mosaic virus* (Uniprot ID: Q90069); TEV, *Tobacco etch virus* (Uniprot ID: P04517); TuMV, *Turnip mosaic virus* (Uniprot ID: Q9ICI2); TVBMV, *Tobacco vein banding mosaic virus* (Uniprot ID: F5A3N8); ZYMV, *Zucchini yellow mosaic virus* (Uniprot ID: P18479); CLV, *Carnation latent virus* (Uniprot ID: A0A858Z687); CMV, *Cucumber mosaic virus* (Uniprot ID: P17769); PSV, *Peanut stunt virus* (Uniprot ID: P28726); TAV, *Tomato aspermy virus* (Uniprot ID: P28931); BYDV, *Barley yellow dwarf virus* (Uniprot ID: P29044); SbDV, *Soybean dwarf virus* (Uniprot ID: A0A6M8PRM6); AMV, *Alfalfa mosaic virus* (Uniprot ID: P03589); PEBV, *Pea early browning virus* (Uniprot ID: Q9WJD8); TRV, *Tobacco rattle virus* (Uniprot ID: Q9J942); PVX, *Potato virus X* (Uniprot ID: A0A7H1C8Y4); TMV, *Tobacco mosaic virus* (Uniprot ID: P03586); TYMV, *Turnip yellow mosaic virus* (Uniprot ID: P10358).

Extended Data Fig. 9 | PVY suppresses plant AD by CI-NAC2 interaction.

a, Alignment of helicase domain from multiple aphid- and non-aphid- transmitted viruses. Asterisk (*) indicates that the Glycine (G) amino acid residue is conserved among listed aphid-transmitted viruses. **b, c,** Accumulation of PVY RNA **(b)** or CP **(c)** in PVY-carrying aphid-attacked leaves of WT receivers (WT-R) with virus-free aphid-attacked WT plants as emitters (AE) or with non-aphid-attacked WT plants as mock emitters (mE) when these receiver plants were fed with PVY-containing aphids. **d, e,**

GC–MS analysis of volatized MeSA in WT plants fed with virus-free aphids or PVY-carrying aphids for 3 days. **f-h,** Accumulation of PVY RNA **(f),** CP **(g)** or proportion of living aphids **(h)** in WT-R plants with PVY-containing aphid-attacked WT plants as emitters (APE) or WT-R (mE) plants when these receiver plants were fed with PVY-containing aphids. **i,** CMV and PVY infection changed NAC2 localization partially to cytoplasm. Scale bar = 25 μm. **j,** BiFC assay showing that PVY CI but not its mutant PVY CI^{G347D} or TMV 126KD, interacted with NAC2. Scale bar = 25 μm. **k,** Immunoblot assay of protein levels in BiFC assay. **l,** PVY CI but not its mutant PVY CI^{G347D} or TMV 126KD, changed NAC2 localization partially to cytoplasm, scale bar = 25 μm. **b, e, f,** Two-sided Student's *t*-test. **h,** One-way ANOVA with LSD. **b, e, f, h,** n=3 biologically independent samples. Data are shown as mean ± s.d.; n.s., no statistical significance. The same letter A represents no statistical difference between samples ($P >$ 0.05). All P values are shown in figure. Experiments were repeated at least three times with similar results.

Extended Data Fig. 10 | Arms race among emitter and receiver plants, aphids, and viruses.

a, AD defends plants against aphids and viruses. When emitter plants are attacked by aphids, they can sense the aphid sap-sucking action and stimulate biosynthesis of SA that activates the NAC2-SAMT1 module to produce volatile MeSA, neighboring receiver plants perceive and convert volatile MeSA into SA by SABP2, which acts as the cue to trigger NAC2-SAMT1 module and elicit defense against aphids and viruses. **b,** Virus and aphid counterdefence. When emitter plants were attacked by viruliferous aphids, some aphid-transmitted viruses utilized their helicase-contained viral protein (for example, CMV1a and PVY CI) to subcellularly re-localize and destabilize NAC2, leading to suppression of NAC2-mediated plant airborne defense to facilitate aphid propagation and virus transmission. The graphical model was created with BioRender.com. In summary, we have exploited interplays among aphid, virus, VOC emitter, and receiver plants in a complexed pathosystem to dissect PPC and AD at genetic and molecular levels. Our study on deciphering AD also lays the

groundbreaking work to empower VOCs as a novel bioinspired tool in defense of plants including agricultural and horticultural crops against insect infestation and virus epidemics.

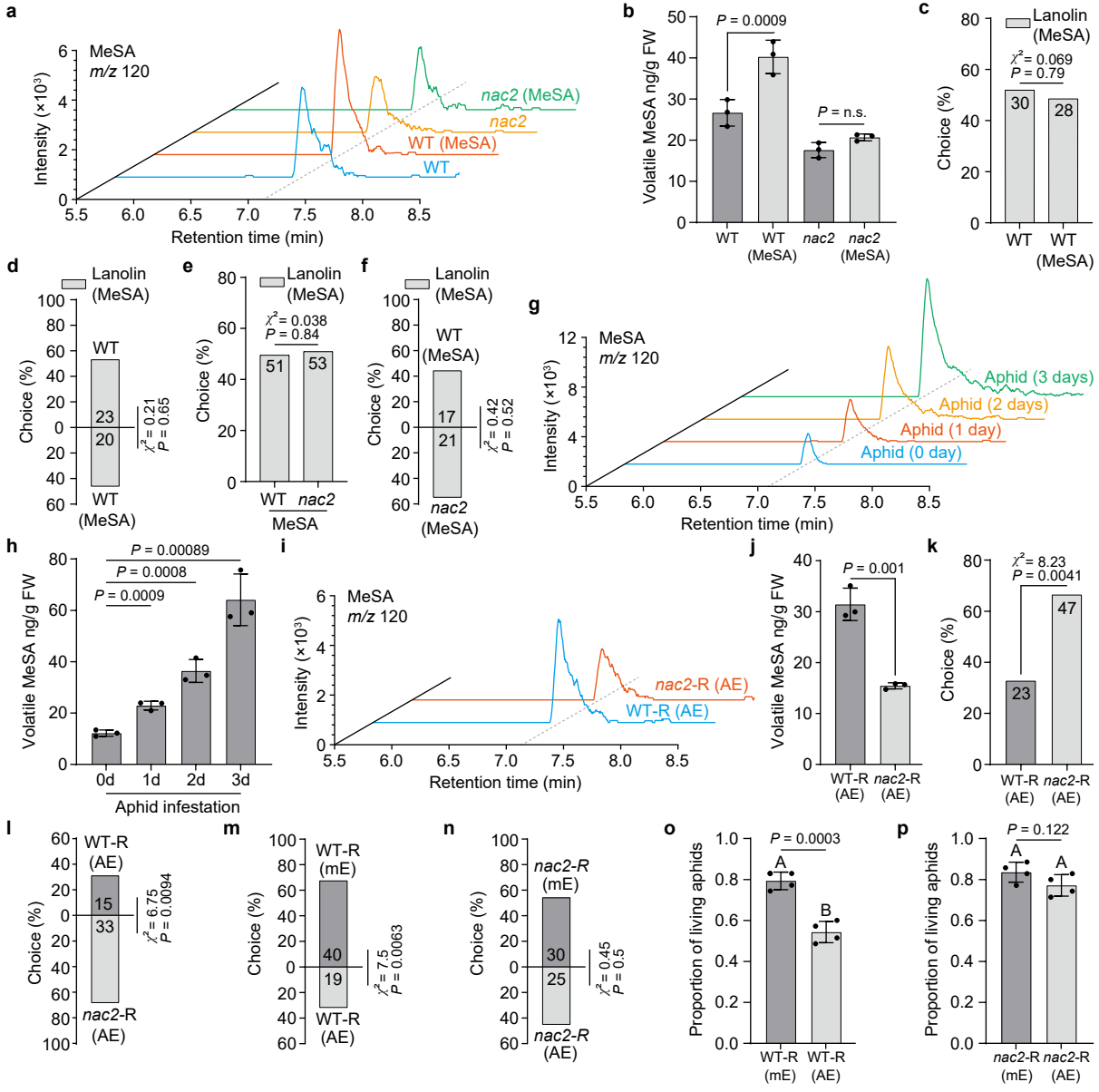
a
MeSA
m/z 120
Intensity (×10³)
Retention time (min)
nac2 (MeSA)
nac2
WT (MeSA)
WT
b
Volatile MeSA ng/g FW
P = 0.0009
P = n.s.
WT
WT (MeSA)
nac2
nac2 (MeSA)
c
Lanolin (MeSA)
χ² = 0.069
P = 0.79
Choice (%)
30
28
WT
WT (MeSA)
d
Lanolin (MeSA)
WT
23
20
WT (MeSA)
χ² = 0.21
P = 0.65
e
Lanolin (MeSA)
χ² = 0.038
P = 0.84
51
53
WT
nac2
MeSA
f
Lanolin (MeSA)
WT (MeSA)
17
21
nac2 (MeSA)
χ² = 0.42
P = 0.52
g
MeSA
m/z 120
Intensity (×10³)
Retention time (min)
Aphid (3 days)
Aphid (2 days)
Aphid (1 day)
Aphid (0 day)
h
Volatile MeSA ng/g FW
P = 0.00089
P = 0.0008
P = 0.0009
0d
1d
2d
3d
Aphid infestation
i
MeSA
m/z 120
Intensity (×10³)
Retention time (min)
nac2-R (AE)
WT-R (AE)
j
Volatile MeSA ng/g FW
P = 0.001
WT-R (AE)
nac2-R (AE)
k
χ² = 8.23
P = 0.0041
Choice (%)
23
47
WT-R (AE)
nac2-R (AE)
l
WT-R (AE)
15
33
nac2-R (AE)
χ² = 6.75
P = 0.0094
Choice (%)
m
WT-R (mE)
40
19
WT-R (AE)
χ² = 7.5
P = 0.0063
Choice (%)
n
nac2-R (mE)
30
25
nac2-R (AE)
χ² = 0.45
P = 0.5
Choice (%)
o
Proportion of living aphids
P = 0.0003
A
B
WT-R (mE)
WT-R (AE)
p
Proportion of living aphids
P = 0.122
A
A
nac2-R (mE)
nac2-R (AE)

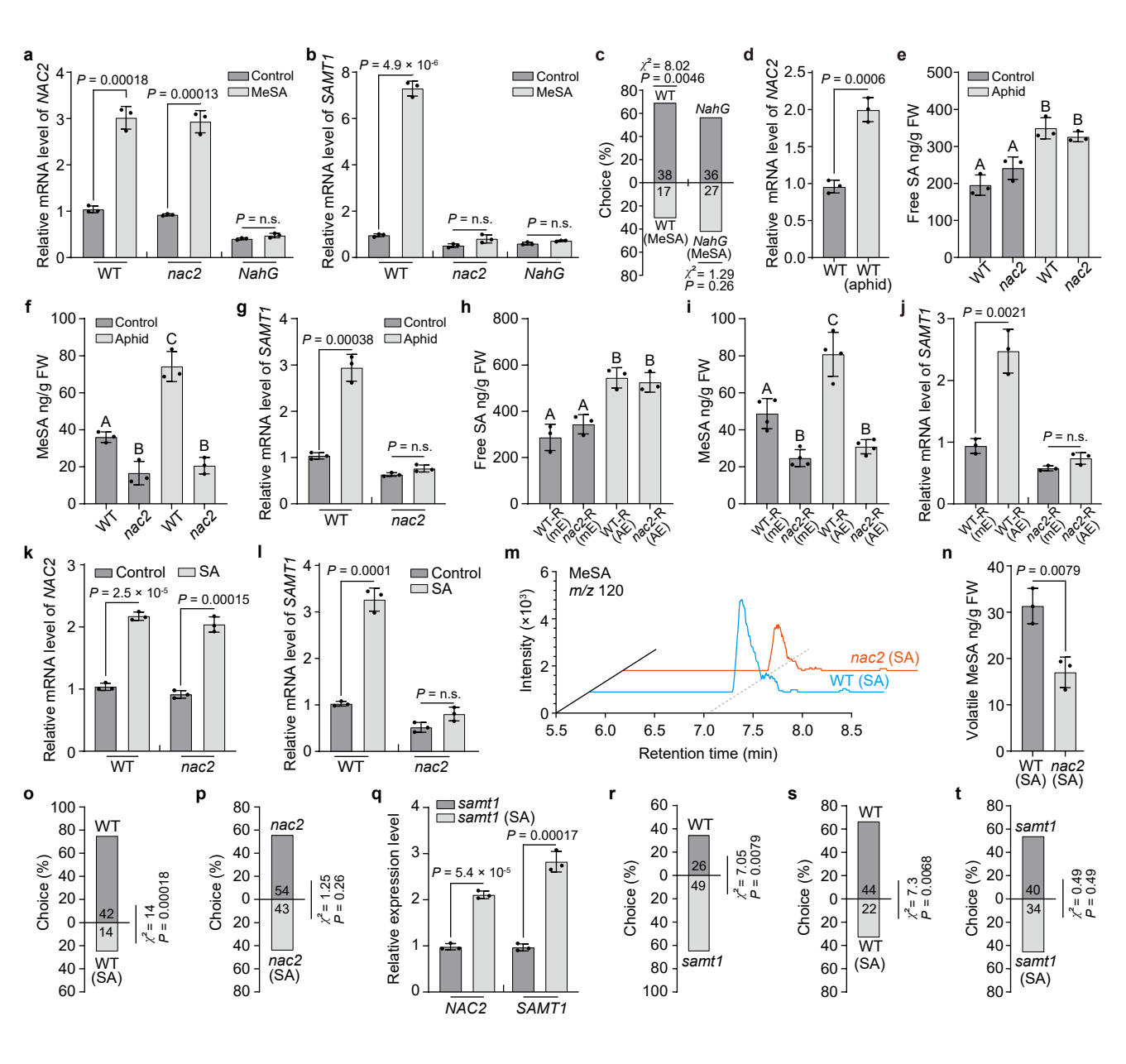
a
Relative mRNA level of NAC2
P = 0.00018
P = 0.00013
P = n.s.
Control
MeSA
WT
nac2
NahG
b
Relative mRNA level of SAMT1
P = 4.9 × 10-6
P = n.s.
P = n.s.
c
χ2 = 8.02
P = 0.0046
Choice (%)
38
17
36
27
χ2 = 1.29
P = 0.26
(MeSA)
d
Relative mRNA level of NAC2
P = 0.0006
WT (aphid)
e
Free SA ng/g FW
Aphid
f
MeSA ng/g FW
g
Relative mRNA level of SAMT1
P = 0.00038
h
Free SA ng/g FW
WT-R (mE)
nac2-R (mE)
WT-R (AE)
nac2-R (AE)
i
MeSA ng/g FW
j
Relative mRNA level of SAMT1
P = 0.0021
k
Relative mRNA level of NAC2
SA
P = 2.5 × 10-5
P = 0.00015
l
Relative mRNA level of SAMT1
P = 0.0001
m
MeSA
m/z 120
Intensity (×10³)
nac2 (SA)
WT (SA)
Retention time (min)
n
Volatile MeSA ng/g FW
P = 0.0079
o
42
14
χ2 = 14
P = 0.00018
p
54
43
χ2 = 1.25
P = 0.26
q
samt1
samt1 (SA)
Relative expression level
P = 5.4 × 10-5
P = 0.00017
NAC2
SAMT1
r
26
49
χ2 = 7.05
P = 0.0079
s
44
22
χ2 = 7.3
P = 0.0068
t
40
34
χ2 = 0.49
P = 0.49

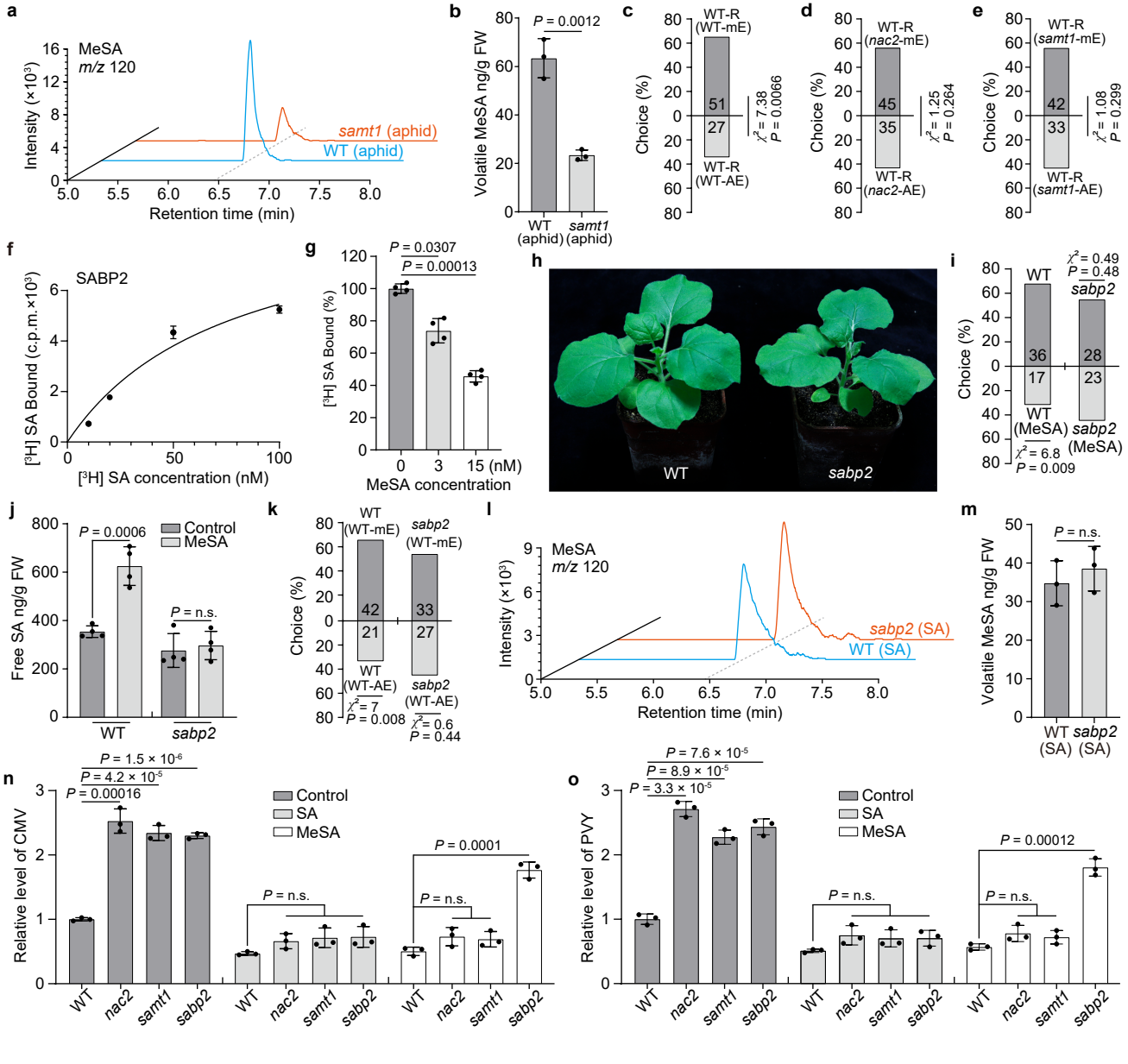
a
MeSA
m/z 120
Intensity (×10³)
samt1 (aphid)
WT (aphid)
Retention time (min)
b
P = 0.0012
Volatile MeSA ng/g FW
WT (aphid)
samt1 (aphid)
c
WT-R (WT-mE)
WT-R (WT-AE)
Choice (%)
χ² = 7.38
P = 0.0066
d
WT-R (nac2-mE)
WT-R (nac2-AE)
χ² = 1.25
P = 0.264
e
WT-R (samt1-mE)
WT-R (samt1-AE)
χ² = 1.08
P = 0.299
f
SABP2
[³H] SA Bound (c.p.m.×10³)
[³H] SA concentration (nM)
g
P = 0.0307
P = 0.00013
[³H] SA Bound (%)
MeSA concentration
h
WT
sabp2
i
χ² = 0.49
P = 0.48
WT (MeSA)
sabp2 (MeSA)
χ² = 6.8
P = 0.009
j
P = 0.0006
P = n.s.
Control
MeSA
Free SA ng/g FW
k
WT (WT-mE)
sabp2 (WT-mE)
WT (WT-AE)
sabp2 (WT-AE)
χ² = 7
P = 0.008
χ² = 0.6
P = 0.44
l
MeSA
m/z 120
sabp2 (SA)
WT (SA)
m
P = n.s.
Volatile MeSA ng/g FW
n
P = 1.5 × 10⁻⁶
P = 4.2 × 10⁻⁵
P = 0.00016
Control
SA
MeSA
Relative level of CMV
P = 0.0001
P = n.s.
o
P = 7.6 × 10⁻⁵
P = 8.9 × 10⁻⁵
P = 3.3 × 10⁻⁵
Relative level of PVY
P = 0.00012

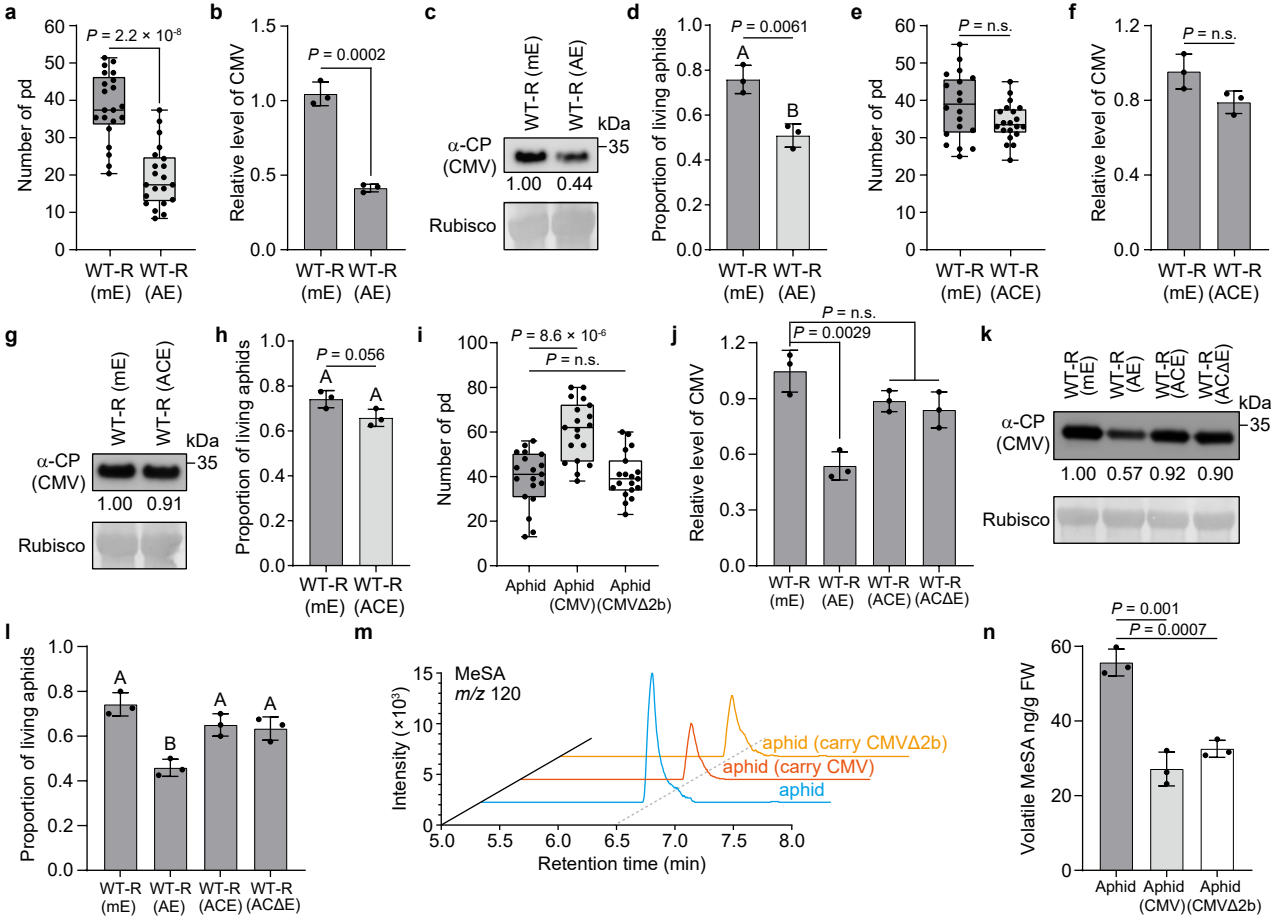
a
Number of pd
P = 2.2 × 10-8
WT-R (mE)
WT-R (AE)
b
Relative level of CMV
P = 0.0002
c
WT-R (mE)
WT-R (AE)
kDa
α-CP (CMV)
35
1.00 0.44
Rubisco
d
Proportion of living aphids
P = 0.0061
A
B
e
Number of pd
P = n.s.
WT-R (ACE)
f
Relative level of CMV
g
WT-R (ACE)
1.00 0.91
h
P = 0.056
i
P = 8.6 × 10-6
Aphid
Aphid (CMV)
Aphid (CMVΔ2b)
j
P = 0.0029
WT-R (ACΔE)
k
1.00 0.57 0.92 0.90
l
m
MeSA
m/z 120
Intensity (×10³)
Retention time (min)
aphid (carry CMVΔ2b)
aphid (carry CMV)
aphid
n
P = 0.001
P = 0.0007
Volatile MeSA ng/g FW